esa ECOSPHERE

Mixing it up in Alaska: Habitat use of adult female Steller sea lions reveals a variety of foraging strategies

Michelle E. Lander,† Brian S. Fadely, Thomas S. Gelatt, Jeremy T. Sterling,
Devin S. Johnson, and Noel A. Pelland

Marine Mammal Laboratory, Alaska Fisheries Science Center, National Marine Fisheries Service, National Oceanic and Atmospheric Administration, Seattle, Washington 98115 USA

Citation: Lander, M. E., B. S. Fadely, T. S. Gelatt, J. T. Sterling, D. S. Johnson, and N. A. Pelland. 2020. Mixing it up in Alaska: Habitat use of adult female Steller sea lions reveals a variety of foraging strategies. Ecosphere 11(2):e03021. 10.1002/ecs2.3021

Abstract. From 2010 to 2015, satellite transmitters were deployed on 16 adult female Steller sea lions (AFSSLs; *Eumetopias jubatus*) in three regions of Alaska because there is limited information regarding the habitat use of this age class during winter and populations have yet to recover in western Alaska. Two approaches were used to assess how static (distance to shore, sea lion site, and continental shelf break, presence on/off the continental shelf, and bathymetric depth and slope), dynamic (proportion of daylight, fraction of lunar illumination, chlorophyll-*a*, wind speed, sea surface height, eddy kinetic energy, and sea surface temperature), and other (region, distinct population segment, and season) covariates affected the habitat use of AFSSLs. Multimodel inference was first used to examine diving behaviors (mean and maximum dive depths, dive frequency) with respect to covariates using linear mixed-effects models, whereas single model inference was used to examine kernel density estimates (KDEs) of individual monthly utilization distributions (n = 74) in western Alaska with respect to environmental covariates using generalized additive models. Additionally, weighted coefficients from these models were examined for the population as a whole, within each individual, between regions, and across monthly scales. Comparisons of foraging behaviors of AFSSLs over time and space revealed pronounced individual variability within overall broader patterns. Response variables of most models were related to various combinations of predictor variables, but distance to shore was the most influential variable across all models. As expected with a non-migratory central place forager, frequency of diving and KDEs were greater on the shelf and near shore, though maximum dive depths increased with distance to shore. Interaction effects (proportion of day light*on/off shelf) observed for mean dive depths suggested AFSSLs were feeding on benthic species when in shelf waters near shore, whereas they were likely feeding on vertically migrating prey species while off-shelf. Relationships regarding diving behaviors and KDEs of AFSSLs relative to dynamic oceanographic variables were not as prominent as those observed for static environmental variables, though some signals were apparent at different scales. Overall, static environmental features likely provided more consistent sources of habitat for prey resources, thereby making them more predictable for AFSSLs.

Key words: diving behavior; *Eumetopias jubatus;* habitat use; kernel density estimator; satellite telemetry; Steller sea lion; utilization distribution.

Received 15 March 2019; revised 17 September 2019; accepted 4 October 2019; final files received 10 December 2019. Corresponding Editor: Hunter S. Lenihan.

† **E-mail:** michelle.lander@noaa.gov

INTRODUCTION

Steller sea lions (SSLs; *Eumetopias jubatus*) inhabit a wide range of oceanic regimes throughout the North Pacific Ocean and adjoining seas, which are characterized by a combination of static and dynamic hydrographic features. Because some of these features constitute essential habitat for prey (e.g., Turner et al. 2017), information regarding those features important to SSLs is necessary for understanding their habitat use, foraging ecology, and the mechanisms that may be influencing their population dynamics (NMFS 2008). Steller sea lions suffered a significant decline in the western area of their U.S. range from the late 1970s through the 1980s (Braham et al. 1980, Loughlin et al. 1992), which led to the species being listed as threatened under the U.S. Endangered Species Act (ESA) during 1990 (55 FR 49204). After two stocks, or distinct population segments (DPS), were identified and geographically delineated at Cape Suckling, Alaska (144° W longitude; Loughlin 1997), the western DPS (wDPS) was subsequently listed as endangered under the ESA during 1997 (62 FR 24345). The wDPS continues to decline west of Samalga Pass (~170° W) in the western and central Aleutian Islands (WAI and CAI; K. Sweeney, *personal communication*), hereafter referred to as western Alaska, whereas the eastern DPS (eDPS) has recovered and was delisted during 2013 (78 FR 66140).

Overall, there have been insufficient data to determine reasons for population declines (NRC 2003), which have varied over time among regions of the SSL metapopulation (York et al. 1996, Loughlin and York 2000). Juvenile mortality was primarily implicated as a factor for steep population declines observed for the wDPS during the 1980s (Merrick et al. 1987, Pascual and Adkison 1994, York 1994, Holmes and York 2003), whereas factors responsible for declines during the 1990s are uncertain (NMFS 2008). Although questionable (Maniscalco et al. 2010, Horning and Mellish 2012), a decline of natality rates appeared to be associated with a paucity of population recovery from the mid-1980s to the early 2000s (Pitcher et al. 1998, Fay and Punt 2006, Winship and Trites 2006, Holmes et al. 2007), but natality rates for the eastern portion of the wDPS have since recovered to baseline rates observed during the early 1970s (Fritz et al. 2014). Lack of vital rates data for western Alaska, however, precludes our understanding of the decline in that area (Fritz et al. 2014).

Reduced pup production may be experienced by adult female Steller sea lions (AFSSLs) suffering from nutritional stress due to prey shortage or quality (Trites and Donnelly 2003), which may be more detrimental to individuals during winter (Rosen 2009). Among other things, lower adult survival may also be a result of food limitation during winter (Altukhov et al. 2015). It is uncertain whether nutritional stress has impeded the recovery of populations in the WAI and CAI, but NMFS (2014) concluded that if nutritional stress is affecting the wDPS, it is probably chronic and due to localized prey limitation and/or low diet diversity. Although the diet of juvenile and AFSSLs has been studied extensively for the wDPS (Sinclair and Zeppelin 2002, Lander et al. 2009, Sinclair et al. 2013, Tollit et al. 2017, Fritz et al. 2019), other aspects of AFSSL foraging ecology that may be representative of their prey base have not been well studied. Diving behaviors and movements of AFSSLs have been described for only a small sample of individuals that were satellite-tagged in the Aleutian Islands and Gulf of Alaska more than 20 yr ago (Merrick et al. 1994, Merrick and Loughlin 1997, Andrews et al. 2002) and habitat use was not quantified thoroughly.

Empirical studies of species–habitat relationships are applicable to the management and conservation of endangered species because they are informative about the biological and physical characteristics of resources and essential features needed to survive, reproduce, and persist (Block and Brennan 1993, Hall et al. 1997). In turn, this knowledge is useful for establishing protected areas for species of concern (Gregr and Trites 2008, Hooker et al. 2011), predicting habitat use with more certainty (Silber et al. 2017), and understanding broader population patterns associated with environmental processes (e.g., Miller et al. 2005, Trites et al. 2007). Additionally, multi-scale approaches for assessing species–habitat relationships have become widely used (Turner 2005, Mayor et al. 2009, McGarigal et al. 2016) in part because animals are thought to interact with their environment across several spatial and temporal scales for different reasons in a hierarchical fashion (Johnson 1980, Wiens 1989). For example, Kalarus and Nowicki (2017) suggested that studies of habitat use conducted over larger spatial scales might reveal drivers of metapopulation dynamics, whereas studies conducted at smaller spatial scales may reveal individual preferences.

The objective of our study was to use a multi-scale framework to assess the winter habitat use of AFSSLs from Alaska. Telemetry studies with AFSSLs have not been conducted since the turn of the century as studies were focused on juveniles because reduced survivorship of this age class was the leading hypothesis for population declines (NMFS 2001). Additionally, ineffective capture techniques, including risks with dart delivery and Telazol complications (Loughlin and Spraker 1989, Heath et al. 1996, Haulena 2007), along with the endangered status of the wDPS, led to a hiatus in research involving the capture of AFSSLs. However, after combinations of chemical immobilizing agents coupled with reversible anesthetic protocols were developed for captive (Spelman 2004, Haulena 2007) and free-ranging (Melin et al. 2013) California sea lions (*Zalophus californianus*), an effective dosage range for the most promising combination of drugs was established for SSLs (Melin et al. 2013, Haulena 2014). To assess the utility of this anesthetic protocol with a remote delivery system for free-ranging AFSSLs, a pilot study was conducted with three individuals in Southeast Alaska (SEAK) due to logistics associated with darting AFSSLs from the wDPS (i.e., ESA status, weather, and accessibility). After successfully darting, tagging, and monitoring those individuals from SEAK, similar protocols were implemented in western Alaska. Two approaches were used to assess the habitat use of AFSSLs from western Alaska, whereby (1) a multimodel inference approach was first used to examine diving behaviors with respect to environmental features, and (2) single model inference was used to examine kernel density estimates (KDEs) of utilization distributions (UDs) with respect to environmental features at various spatial and temporal scales.

METHODS

Captures

Three AFSSLs associated with a pup or juvenile were chemically immobilized at three haulout sites in SEAK (eDPS) during November 2010 (Table 1 and Fig. 1) using darting techniques (Appendix S1). All AFSSLs were measured, weighed, sampled, and Fastloc-GPS satellite transmitters (SPLASH10-F-400, Wildlife Computers, Redmond, Washington, USA), hereafter referred to as “tags,” were attached to the head of each animal using 5-min epoxy (Devcon, Riviera Beach, Florida, USA) prior to administration of reversal drugs and release (Appendix S1).

After anesthetic protocols were administered safely to SEAK individuals, 13 AFSSLs of the wDPS from western Alaska ($n = 3$ in the WAI and $n = 10$ in the CAI) were darted and tagged at seven rookeries and two haulout sites during October–November from 2011 to 2015 (Table 1, Fig. 1, and Appendix S2: Figs. S1−S2). All tags were programmed to acquire Fastloc-GPS positions every 15 min and conductivity (wet/dry) readings every 20 min, which were compiled into 24-h timeline messages. From 2010 to 2014, tags were programmed to transmit dive histogram messages, whereas during 2015, tags were programmed to transmit dive behavior messages. For dive histogram messages, maximum dive depths were summarized for 14 bins, over four 6-h periods per day (00:00–5:59, 6:00–11:59, 12:00–17:59, 18:00–23:59 Greenwich Mean Time; Appendix S1). Dive behavior messages included maximum depth of individual qualifying dives (defined as ≥10 m depth and ≥1-min duration) and the time at which they occurred.

Data analyses

All telemetry data were obtained from the Argos Data Collection and Location System, decoded, cleaned, speed filtered, projected, and processed with a continuous-time correlated random walk (CTCRW) model to predict animal locations corresponding to the 20-min timeline data, followed by a land-avoidance algorithm (Appendix S1).

*Dive histogram data.—*Summary statistics (i.e., mean maximum dive depth; hereafter mean dive depth, maximum dive depth, and number of dives) for dive depth bin data >4 m (Merrick

Table 1. Capture data and post-release monitoring information for 16 AFSSLs satellite-tagged in Alaska from 2010 to 2015.

AFSSL #	Date capture	Location capture	Region	Mass (kg)	SL (cm)	Girth (cm)	Tracking days
eDPS							
61079	11/04/2010	Benjamin Isl.	SEAK	205.5	214.0	138.0	252
61111	11/06/2010	SW Brothers Isl.	SEAK	237.5	224.5	173.0	267
61083	11/07/2010	Sail Isl.	SEAK	211.0	217.0	144.0	200
wDPS							
35224	11/01/2011	Hasgox Pt., Ulak Isl.	CAI	360.0	268.0	172.0	174
14751	10/18/2012	Cape Wrangell, Attu Isl.	WAI	. . .	235.0	152.0	225
61087	10/20/2012	Alaid Isl.	WAI	336.0	257.0	169.5	18
61142	10/23/2012	Cape Sabak, Agattu Isl.	WAI	353.5	258.0	177.0	252
61089	10/25/2012	East Cape, Amchitka Isl.	CAI	340.0	235.0	177.0	46
61080	10/26/2012	Hasgox Pt., Ulak Isl.	CAI	323.0	242.0	165.0	149
61095	10/03/2014	Cape St. Stephen, Kiska Isl.	CAI	352.0	259.0	170.0	252
35226	10/04/2014	Lief Cove, Kiska Isl.	CAI	353.5	255.0	168.0	223
34449†	10/08/2014	Lake Point, Adak Isl.	CAI	365.0	252.0	193.0	96
35222	10/04/2015	East Cape, Amchitka Isl.	CAI	347.5	272.0	155.5	33
61081	10/05/2015	Hasgox Point, Ulak Isl.	CAI	223.0	235.0	142.0	15
61088	10/05/2015	Hasgox Point, Ulak Isl.	CAI	380.5	268.0	177.5	222
61105	10/06/2015	Ship Rock, Kanaga Isl.	CAI	371.0	269.0	171.0	202

Notes: AFSSLs, adult female Steller sea lions; CAI, central Aleutian Islands; eDPS, eastern distinct population segment; SEAK, Southeast Alaska; SL, standard length; WAI, western Aleutian Islands; wDPS, western distinct population segment. Ellipses indicate no data.

† Transmissions were initiated on 12/11/2014 (instead of capture date) because this individual was also tagged with a prototype transmitter (see Lander et al. 2015).

Fig. 1. Locations where 16 adult female Steller sea lions (AFSSLs) were captured in the western and central Aleutian Islands (WAI, CAI) and Southeast Alaska (SEAK) from 2010 to 2015. The scale bar is for the larger base map (Ocean Basemap Sources: Esri, GEBCO, NOAA, National Geographic, DeLorme, HERE, Geonames.org, and other contributors).

et al. 1994, Loughlin et al. 2003) were calculated for each histogram message using methods of Lea et al. (2010) and assigned to the CTCRW predicted spatial location corresponding to the temporal midpoint of each dive period. Categorical covariates (i.e., geographic region, DPS, and two definitions of seasons) were assigned to each wet spatial location associated with dive data and a series of static and dynamic environmental covariates were extracted for those locations (Appendix S1). Static environmental variables included bathymetric depth and two measures of bathymetric slope (i.e., degrees and percent rise; PR). Additionally, distances to shore, nearest SSL site (including rookeries and haulouts), and continental shelf break (200 m bathymetric contour) were calculated for each dive location, which was also categorized as being on or off the shelf.

Proportion of daylight per 6-h period and daily fraction of lunar illumination were extracted for all dive locations as described in Sterling et al. (2014), whereas other dynamic environmental variables, including chlorophyll-*a* (chl-*a*), wind speed, sea surface height (SSH), eddy kinetic energy (EKE), and sea surface temperature (SST), were only extracted for dive locations from the wDPS dataset because remote sensing data from SEAK are unreliable due to topographic effects of the coast and shelf in that area. Additionally, local artifacts associated with coastal data tend to distort altimetry signals and can produce unrealistic features (Caballero et al. 2008). For visualization purposes, geoprocessing tools (Appendix S1) were used to determine the core location and polarity of geostrophic eddies (Henson and Thomas 2007) in daily SSH rasters using the Okubo-Weiss (OW) parameter (Okubo 1970, Weiss 1991) with default threshold values.

Dive data summary statistics were log-transformed and used as response variables in linear mixed-effect (LME) models (nlme package, R 3.0.1, R Development Core Team 2016) with individual as a random effect/grouping variable and a first-order autoregressive [AR(1)] correlation structure. The random intercepts and AR (1) correlation structure within each animal accounted for both pseudo-replication of dive periods by fitting an effect to control for overall diving differences between individuals and for temporal similarity of dive periods within each individual's time series. These models were examined for two distinct groups. For one group, both stocks were pooled and response variables were examined relative to all categorical and static environmental covariates and some dynamic environmental covariates (i.e., proportion of daylight and fraction of lunar illumination) because the remaining dynamic environmental covariates were not extracted for the eDPS AFSSLs. For the second group, response variables were examined with respect to all covariates for AFSSLs from only the wDPS. Model selection initially entailed examining each of the three response variables relative to independent predictor variables, including two interaction terms (i.e., proportion of daylight * presence on/off the shelf, lunar fraction * presence on/off the shelf). Region and season were coded as indicator variables with the WAI and winter used as controls, respectively. Significant covariates and interaction terms from the independent models were then used to construct a full model for each dive response variable. Akaike information criterion (AIC) was used to choose the best covariate for full models in cases where there was more than one measurement for a given covariate (i.e., season and bathymetric slope) or covariates were similar or correlated (i.e., distance to shore and distance to nearest SSL site). All full models served as the initial model for backward stepwise model selection using AIC (stepAIC, package MASS, R), and diagnostic plots (i.e., q-q and residuals) were used to determine whether those models were appropriate. Additionally, plots were examined to interpret interaction effects. Lastly, a significance level of $P \leq 0.05$ was used for all LME analyses.

*Dive behavior data.—*After extracting environmental covariates for each spatially explicit dive location (Appendix S1), these data were analyzed using LME models as described above, except dives were classified as day or night (in lieu of proportion of daylight per 6-h period). Interaction effects were not examined due to the limited sample size. To discern benthic foraging, a dive index (DI) ratio was calculated for each dive by dividing maximum dive depth by corresponding bathymetry value (Simmons et al. 2007) and dives with DI values ≥0.95 were classified as benthic dives (Jessopp et al. 2013).

Kernel density estimators.—To examine the relative intensity of spatial habitat use by AFSSLs from the wDPS, wet predicted locations generated from the CTCRW models were used to construct monthly UDs for each individual (Van Winkle 1975, Worton 1989) using kernel density estimators (Appendix S1). For qualitative purposes (i.e., visual interpretation via data overlay), polygons representing the 0.95 and 0.50 quantiles of each monthly grid were constructed to define home range and core areas, respectively (Van Winkle 1975, Samuel et al. 1985, Laver and Kelly 2008).

Following data adjustment, covariate extraction, and collinearity diagnostics (Appendix S1), KDEs of monthly UDs were log-transformed and examined with respect to seven environmental covariates (i.e., distance to shore and shelf break, bathymetric depth and slope, SST, SSH, and EKE) using individual-based generalized additive models with a Gaussian distribution and restricted maximum likelihood (REML; mgcv package, R; Wood 2006, 2009). To address spatial autocorrelation in the data, a smooth function was applied to the spatial coordinates of each observation (i.e., centroid of UD grid cells) as an additional predictor variable in each individual-based monthly generalized additive model (IMGAM). Basis function size (k) of the spatial term for each IMGAM was increased by a factor of 10 until the gam.check function in the mgcv package indicated the k-index value was ≥1.0 (Wood 2017). Function bam with fast REML (fREML) was used for larger datasets that needed longer computational time due to greater k values (e.g., $k > 100$; Wood et al. 2015).

Unlike the multimodel inference approach used for the dive data, predictor variables of IMGAMs were the same across individuals and months to reduce computing times (Ver Hoef and Boveng 2015) and so results could be summarized collectively at different spatial and temporal scales. For each predictor variable, IMGAM coefficients ($\hat{\beta}$) were pooled across four different groupings of the data, including the population as a whole, and within each individual, region (WAI and CAI), and month (October–June). The weighted population mean ($\bar{\beta}$) of each group was calculated using the following:

$$\bar{\beta} = \sum_{i=1}^{n} w_i \hat{\beta}_i,$$

where the weight (ω) for each coefficient estimate ($\hat{\beta}$) was proportional to 1/Var ($\hat{\beta}_i$). Additionally, the standard error (SE) of each group ($\bar{\beta}$) was calculated using the following:

$$\mathrm{SE}\ (\bar{\beta}) = \sqrt{\sum_{i}^{n} w_i^2 \times \mathrm{Var}(\hat{\beta}_i)}$$

to determine whether $\bar{\beta}$ for each covariate differed from zero. Standard errors also were used to compare the significance of $\bar{\beta}$ estimates between regions and among months, where estimates were considered different if SEs did not overlap.

Because distance to shore was the primary predictor variable found to influence the distribution of AFSSLs across datasets (see *Results*), a subset of off-shelf UDs corresponding to wet, predicted locations beyond the continental shelf were computed for six AFSSLs to further investigate which environmental features were influencing the distribution of AFSSLs in off-shelf waters (Appendix S1). Analyses described above were repeated using single model inference with the same environmental predictor variables. Results of IMGAMs were not compared between regions because only one individual traveled off-shelf in the WAI. Additionally, monthly comparisons of pooled IMGAMs did not extend beyond April.

RESULTS

Following chemical immobilization, all AFSSLs were found at a deep plane of anesthesia and all vital signs were within normal ranges during sampling and tagging procedures (Appendix S2: Fig. S2). After reversal drugs were administered, all AFSSLs were awake and active in <15 min and post-release behaviors were monitored up to ~9 months (Table 1).

Tags transmitted for an average ± SD of 164 ± 92 d (range = 15–267; Table 1), during which time an average of 2047 ± 1415 GPS locations per individual were collected (range = 200–5545). Cleaning and speed filtering the data resulted in an average of 1672 ± 1149 GPS locations per individual (range = 158–4326), for a total of 26,744 locations. Applying the CTCRW model and land-avoidance algorithm to the filtered telemetry dataset resulted in 135,491 (n = 34,512 eDPS, 100,979 wDPS) wet, predicted positions for 20-min intervals for all 16 animals ($\bar{x}$ = 8468 positions per individual, SD = 4728, range = 822–14,716; Figs. 2, 3). For the wDPS dataset, 17,598 positions occurred off-shelf for six animals (#35222, #35224, #35226, #61080, #61089, and #61142).

AFSSL movements

In SEAK, #61079 remained around Benjamin Island, within Favorite Channel in upper Lynn Canal until April before proceeding into Berners Bay and northern inlets through May. Thereafter,

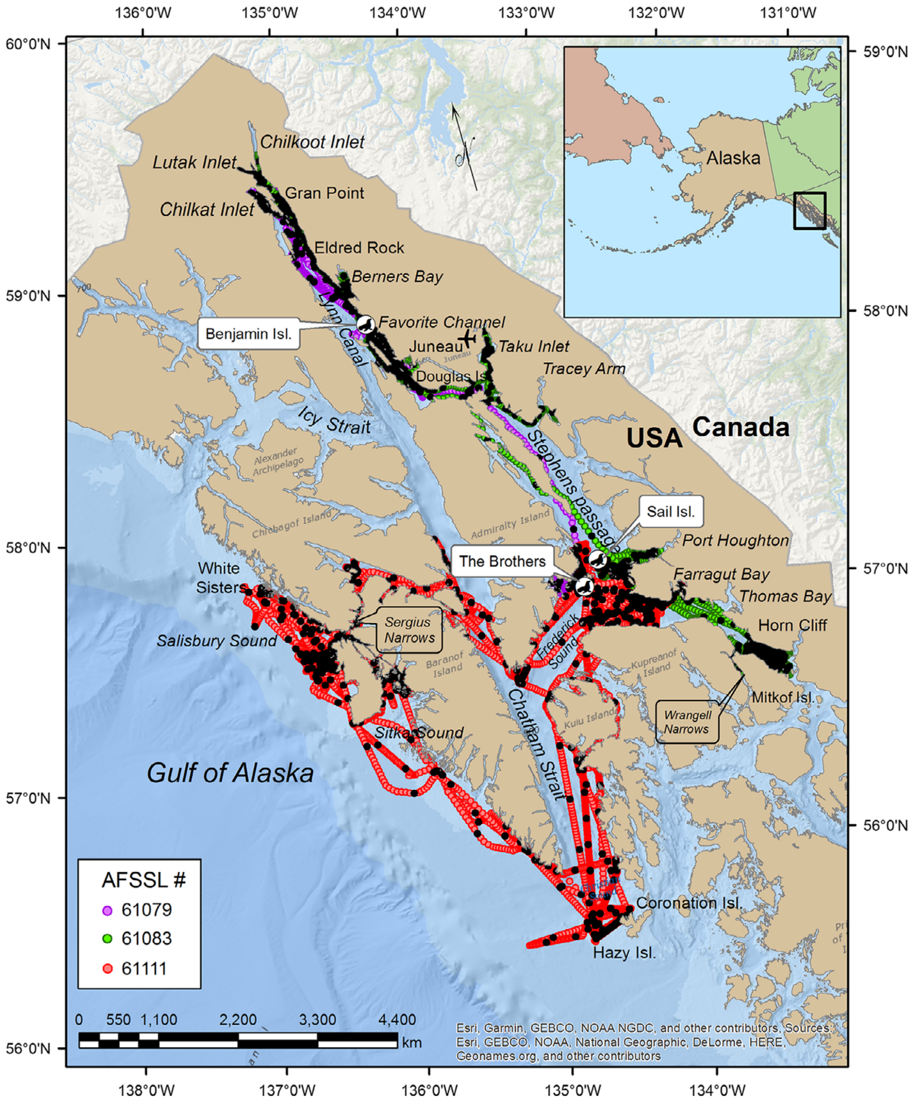

Fig. 2. Wet, predicted locations (n = 34,512) from continuous-time correlated random walk (CTCRW) models for three AFSSLs from the eastern distinct population segment (DPS) in SEAK. Black dots (n = 1565) represent positions corresponding to the temporal midpoint of each daily 6-h period, where dive histogram data (mean, maximum, and frequency of maximum dive depths) were assigned and environmental covariates were extracted.

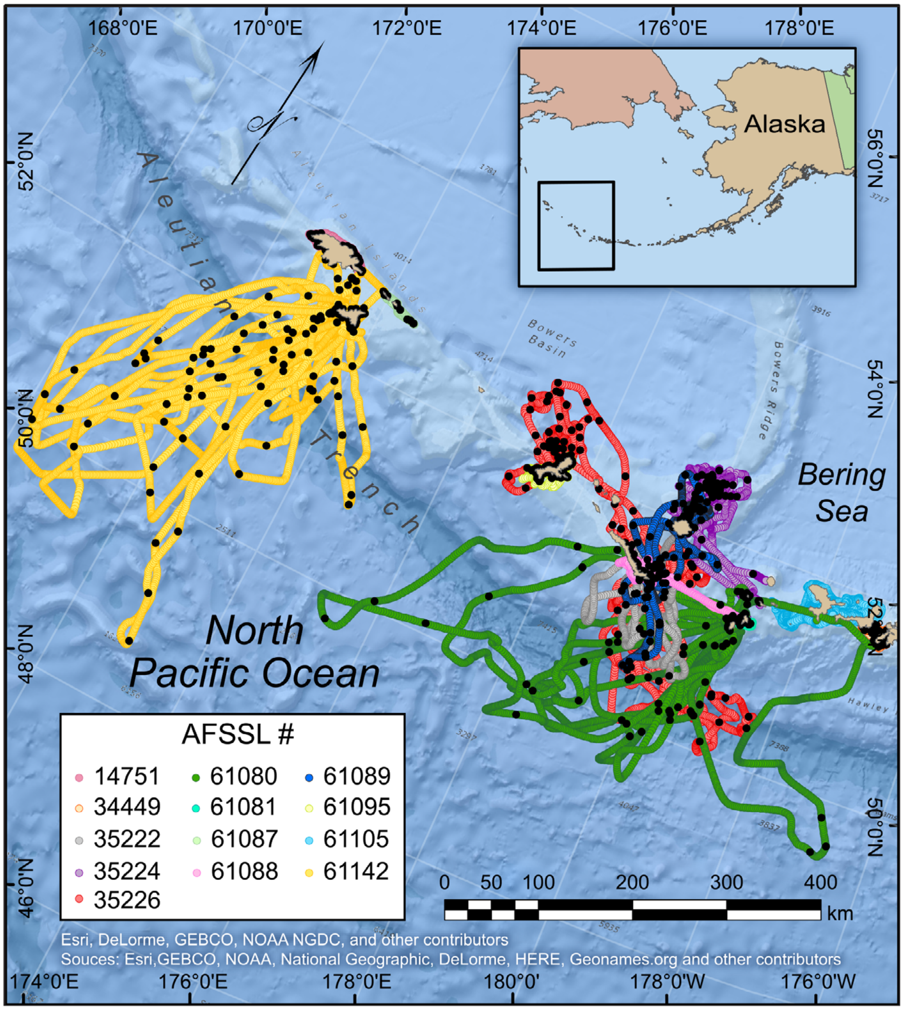

Fig. 3. Wet, predicted locations (n = 100,979) from CTCRW models for 13 AFSSLs from the western DPS in the Aleutian Islands. Dive histogram locations (n = 1615) are illustrated, whereas locations of dives (n = 20,941) from behavior messages for three AFSSLs (#35222, #61088, and #61105) are not included because they covered the tracks.

all movements ranged between Benjamin Island and northern sites until July, when she traveled south to Frederick Sound until signal cessation on 15 July (Fig. 2). Until mid-February, #61083 used areas around Frederick Sound, including Port Houghton, some smaller bays, and a trip into the Wrangell Narrows, after which she moved up to Favorite Channel until mid-April. Thereafter, #61083 proceeded to use similar areas as #61079 for the remainder of tag life (end of May), but also made a trip back down to Taku Inlet and Tracey Arm during April. In contrast, #61111 only remained in Frederick Sound until December before embarking on a series of looping trips, whereby she headed north into the inside passage, traveled through Sergius Narrows, and exited Salisbury Sound into coastal waters of the Gulf of Alaska. Once on the outer coast, she traveled to Sitka Sound and multiple SSL haulouts before heading back through Chatham Strait and into Frederick Sound to repeat the process.

In western Alaska, seven (#14751, #34449, #61081, #61087, #61088, #61095, and #61105) of 13

AFSSLs remained primarily on the continental shelf and close to shore for tag duration, whereas six AFSSLs used both shelf and off-shelf habitats, traveling as far as 420 km from shore (Fig. 3). All but one of those AFSSLs (#35224) traveled south of the Aleutian Archipelago into waters of the North Pacific Ocean, either near or beyond the Aleutian Trench. Three AFSSLs (#35224, #35226, and #61089) used off-shelf areas in the western Bering Sea Basin (Bower's Basin) and Petrel Bank, northwest of Semisopochnoi Island in the CAI. The majority of locations occurred back on the shelf by April for those off-shelf AFSSLs with tags that transmitted beyond winter (#34224, #35226, and #61142). All AFSSLs remained in their region of capture.

Dive data

*Dive histograms.—*A total of 3669 histograms had maximum dive depths (n = 264,124; Table 2) exceeding 4 m (Appendix S1), which averaged 28.4 ± 36.0 m. After interpolating dive summary statistics to CTCRW positions, 3180 histograms were associated with wet, predicted locations (Table 2; Figs. 2, 3) and maximum depths of dives (n = 249,014) averaged 29.2 ± 36.6 m.

*Mixed-effects models (pooled stocks).—*Significant relationships were found for the majority of models (n = 31) when individual dive response variables were examined with respect to independent covariates for the pooled dataset comprised of both stocks (Appendix S3: Table S1). Lunar fraction and bathymetric slope (PR) were the only covariates that were not significant predictors of any dive response variables. AIC values indicated calendar season was a better predictor of diving behaviors than two seasons (winter/summer) for two (i.e., mean and maximum dive depths) of the three response variables. Likewise, DPS was a better model fit than region for mean maximum dive depths and number of dives (i.e., dive frequency). Distance to shore had lower AIC values than distance to nearest SSL site for all three dive variables, and bathymetric slope as calculated in degrees had lower AIC values than calculated as PR for the majority of response variables (Appendix S3:

Table 2. Summary statistics for maximum dive depths obtained from histogram messages (n = 3669) for 13 AFSSLs and dive profiles (n = 21,644) for three AFSSLs, as well as the subset of dive histograms (n = 3180) and profiles (n = 20,941) interpolated to wet, predicted locations from CTCRW models.

	All Histogram messages				CTCRW Histogram messages			
AFSSL #	# Histos	# Dives	$\bar{x}$ ± SD (m)	Range (m)	# Histos	# Dives	$\bar{x}$ ± SD (m)	Range (m)
eDPS								
61079	679	49,832	46.6 ± 37.0	5–250	620	47,929	47.5 ± 37.0	5–250
61111	534	32,423	34.2 ± 40.4	5–250	464	30,559	34.9 ± 40.8	5–250
61083	539	31,291	56.9 ± 55.6	5–250	481	30,049	58.2 ± 56.0	5–250
wDPS								
35224	145	5693	31.9 ± 57.0	5–250	134	5428	32.9 ± 58.2	5–250
14751	264	23,021	12.5 ± 7.8	5–62	241	22,222	12.6 ± 7.9	5–62
61087	22	1648	12.7 ± 7.8	5–42	18	1575	12.7 ± 7.6	5–42
61142	243	14,143	17.5 ± 19.3	5–187	217	13,535	17.7 ± 19.6	5–187
61089	51	3355	13.5 ± 15.8	5–187	46	3149	13.9 ± 16.2	5–187
61080	132	7532	22.0 ± 26.2	5–250	111	6969	22.6 ± 26.9	5–250
61095	430	44,164	11.7 ± 8.9	5–112	311	39,505	11.8 ± 9.1	5–112
35226	409	38,734	12.1 ± 12.1	5–162	362	36,842	12.2 ± 12.3	5–162
34449	195	10,511	27.4 ± 28.7	5–187	154	9498	29.0 ± 29.6	5–187
35222†	. . .	1085	48.9 ± 35.2	10–327.8	. . .	1075	49.2 ± 35.2	10–327.8
61081	26	1777	32.1 ± 29.9	5–187	21	1754	32.4 ± 29.9	5–187
61088†	. . .	10,910	22.5 ± 15.3	10–631.8	. . .	10,458	22.6 ± 15.5	10–631.8
61105†	. . .	9, 649	33.8 ± 24.3	10–215.8	. . .	9408	34.1 ± 24.4	10–215.8

Notes: CTCRW, continuous-time correlated random walk; Histos, histogram messages; $\bar{x}$ ± SD, mean of maximum dive depths ± standard deviation; m, meters. Other abbreviations and symbols are as in Table 1.

† Dive profiles (as opposed to histograms) were collected for these individuals.

Table S1). Consequently, calendar season, DPS, distance to shore, and slope degrees were used in all full models (Table 3).

Overall, full models provided best model fits as no covariates were eliminated during stepwise analyses. Mean depths of dives during winter were significantly deeper than during all other seasons, whereas maximum depths of dives during winter only exceeded those during summer (Table 3). Dive frequency during spring and summer was greater than during winter. Furthermore, mean and maximum dive depths of AFSSLs from SEAK (eDPS) were greater than those of AFSSLs from the Aleutian Islands (wDPS). Mean and maximum dive depths were positively related to distance to shore (and

Table 3. Results of stepwise LME models used to examine diving behaviors (i.e., mean, maximum, and number of maximum dive depths from histogram messages) of 13 AFSSLs from the eDPS (n = 3) and wDPS (n = 10) with respect to covariates that were significant for independent LME models.

Covariate	# Groups	# Obs	AIC	Value	SE	DF	*t*-value	*P*
Mean Max Dive Depth	13	3166	5854.068					
(Intercept)***				3.8448	0.1409	3143	27.2810	0.0000
C Season (spring)***				−0.2076	0.0414	3143	−5.0172	0.0000
C Season (summer)***				−0.6679	0.0840	3143	−7.9506	0.0000
C Season (fall)***				−0.1359	0.0387	3143	−3.5098	0.0005
DPS (western)***				−1.0358	0.1485	11	−6.9756	0.0000
Dist to shore (m)***				2.300^{-5}	1.830^{-6}	3143	12.5025	0.0000
Dist to shelf break (m)***				-2.300^{-5}	1.960^{-6}	3143	−11.7710	0.0000
Shelf (on)***				0.2767	0.0600	3143	4.6140	0.0000
Bathymetric depth (m)				3.700^{-5}	2.216^{-5}	3143	1.6728	0.0945
Bathymetric slope (°)***				−0.0054	0.0016	3143	−3.4227	0.0006
Prop day				0.0955	0.0648	3143	1.4736	0.1407
Prop day: shelf (on)***				−0.5103	0.0701	3143	−7.2798	0.0000
Max Dive Depth	13	3,167	5683.978					
(Intercept)***				5.0029	0.1379	3145	36.2851	0.0000
C Season (spring)				−0.0039	0.0384	3145	−0.1023	0.9185
C Season (summer)***				−0.3845	0.0779	3145	−4.9352	0.0000
C Season (fall)				−0.0277	0.0359	3145	−0.7706	0.4410
DPS (western)***				−0.9159	0.1460	11	−6.2738	0.0001
Dist to shore (m)***				2.200^{-5}	1.750^{-6}	3145	12.4880	0.0000
Dist to shelf break (m)***				-2.200^{-5}	1.870^{-6}	3145	−11.5666	0.0000
Shelf (on)				−0.0379	0.0585	3145	−0.6479	0.5171
Bathymetric depth (m)***				0.0001	2.130^{-5}	3145	3.3464	0.0008
Prop day***				−0.2719	0.0635	3145	−4.2783	0.0000
Prop day: shelf (on)*				−0.1606	0.0686	3145	−2.3399	0.0194
No. of Dives	13	3167	7541.658					
(Intercept)***				4.1435	0.1193	3145	34.7395	0.0000
C Season (spring)***				0.3303	0.0465	3145	7.1105	0.0000
C Season (summer)***				0.6646	0.0937	3145	7.0907	0.0000
C Season (fall)				−0.0606	0.0430	3145	−1.4077	0.1593
Dist to shore (m)*				-5.000^{-6}	2.260^{-6}	3145	−2.0789	0.0377
Dist to shelf break (m)*				6.000^{-6}	2.430^{-6}	3145	2.3737	0.0177
Shelf (on)*				0.1630	0.0788	3145	2.0673	0.0388
Bathymetric depth (m)*				-6.300^{-5}	2.767^{-5}	3145	−2.2837	0.0225
Prop day***				−0.3403	0.0867	3145	−3.9227	0.0001
Prop day: shelf (on)***				−0.3867	0.0936	3145	−4.1328	0.0000

Notes: AIC, Akaike information criterion; C, calendar; °, degrees; DF, degrees freedom; Dist, distance; LME, linear mixed-effects; Obs, observations; Prop day, proportion of daylight per 6-h dive histogram period; SE, standard error; Shelf, presence on (vs. off) the continental shelf (200 m); Value, coefficient value. Other abbreviations are as in Tables 1, 2. Significant covariates from independent LME models (Appendix S3: Table S1) were used to construct full models for stepwise analyses.

*$P < 0.05$, **$P < 0.01$, ***$P < 0.001$.

bathymetry for maximum dive depths), whereas dive frequency was negatively related to distance to shore and bathymetry. Mean dive depths displayed a negative relationship with bathymetric slope. Lastly, negative relationships were found between mean and maximum dive depths and distance to the shelf break, whereas frequency of diving increased with distance to the shelf break (Table 3).

Significant interactions between proportion of daylight and foraging location (on/off the shelf) were found for all three dive response variables. Mean dive depths were deeper during night than during the day when AFSSLs were in shelf waters, whereas mean dive depths did not vary significantly with proportion of daylight while in off-shelf waters. Maximum dive depths and dive frequency were negatively related to proportion of daylight both on and off the shelf.

Mixed-effects models (western DPS).—Similar to the pooled dataset, significant relationships were found for most models when dive response variables were examined with respect to independent static environmental covariates for the wDPS (Appendix S3: Table S2). In contrast, only a few significant relationships were found when mean and maximum dive depths were examined with respect to independent dynamic environmental covariates, whereas that was not the case for dive frequency. Season as represented by two periods (winter/summer) was a better predictor of dive response variables than calendar season based on AIC values, but calendar season was used in full models to be consistent with the pooled dataset.

Stepwise analyses of full models for the wDPS indicated all response variables were significantly related to a combination of the following predictor variables: season, distance to shore and shelf break, presence on/off the continental shelf, SST, fraction of lunar illumination, proportion of daylight, and some interaction effects (Table 4). Eddy kinetic energy, which was included as a covariate in full models for mean and maximum dive depths, was eliminated during the selection process, whereas no covariates were eliminated for the dive frequency full model. Unlike the pooled dataset, season was only a significant predictor covariate for maximum dive depths, which increased during fall and spring (relative to winter). Independent of other covariates, diving was deeper as animals traveled further from shore and into warmer waters, though the effect of distance to shore was counteracted by distance from shelf break for animals that were off-shelf. A negative lunar effect was evident for maximum dive depths. Although AFSSLs primarily were nocturnal foragers, mean dive depths were deeper during the night than during the day when they were in waters over the continental shelf, whereas the opposite occurred when they were in off-shelf waters. Maximum dive depth was negatively related to proportion of daylight while on the shelf, whereas dive frequency was negatively related to proportion of daylight both on and off-shelf.

Dive behaviors (western DPS).—Overall, maximum depths of dive profiles (*n* = 21,644; Table 2) for three CAI AFSSLs (#3522, #61088, and #61105) averaged 28.9 ± 22.2 m. After interpolating dives to CTCRW positions, 20,941 dives were associated with wet, predicted locations and joined with environmental covariates. Similarly, maximum depths of dives for this subset of data averaged 29.1 ± 22.4 m. The majority of dives (99.5% and 95.5%) occurred in shelf waters for #61088 and #61105, respectively. In contrast, the majority of dives (68.2%) occurred in off-shelf waters for #35222. The majority (82%) of dives for all three AFSSLs occurred during night. Dives missing bathymetry data (*n* = 146) were not assigned a DI value; otherwise, DI values indicated benthic dives were confined to the shelf and comprised 12.4%, 69.5%, and 61.3% of dives for #35222 (*n* = 1073), #61088 (*n* = 10,425), and #61105 (*n* = 9297), respectively.

Independent LME model results indicated relationships between maximum dive depths and static environmental covariates, lunar fraction, and daylight (Appendix S3: Table S3) were similar to results found for maximum dive depths from the wDPS histogram dataset (Appendix S3: Table S2). Unlike the latter dataset, SST was not significant or included in the full model for the stepwise analysis. Results of that analysis (Table 5) also were similar to those found for histogram maximum dive depths (Table 4), except EKE (of opposite sign) was retained in the final model. Similar results between the two datasets were reassuring, given the dive summary statistics from histogram

Table 4. Results of stepwise LME models used to examine diving behaviors (i.e., mean, maximum, and number of maximum dive depths from histogram messages) of 10 AFSSLs from the wDPS with respect to covariates that were significant for independent LME models.

Covariate	# Groups	# Obs	AIC	Value	SE	DF	*t*-value	*P*
Mean Max Dive Depth	10	831	1470.899					
(Intercept)***				2.7557	0.1125	814	24.4912	0.0000
Dist to shore (m)***				1.940^{-5}	2.140^{-6}	814	9.0925	0.0000
Dist to shelf break (m)***				-1.900^{-5}	2.270^{-6}	814	−8.4703	0.0000
Shelf (on)***				0.3646	0.0800	814	4.5562	0.0000
SST (°C)*				0.1019	0.0461	814	2.2121	0.0272
Lun illum				−0.1049	0.0698	814	−1.5020	0.1335
Prop day***				0.5719	0.0757	814	7.5574	0.0000
Prop day: shelf (on)***				−1.0030	0.0955	814	−10.5067	0.0000
Max Dive Depth	10	831	1550.347					
(Intercept)***				4.3093	0.1180	811	36.5067	0.0000
C Season (spring)***				0.3745	0.0847	811	4.4186	0.0000
C Season (summer)				0.2802	0.2742	811	1.0216	0.3073
C Season (fall)**				0.1874	0.0699	811	2.6797	0.0075
Dist to shore (m)***				1.500^{-5}	2.210^{-6}	811	6.9736	0.0000
Dist to shelf break (m)***				-1.400^{-5}	2.330^{-6}	811	−6.0483	0.0000
Shelf (on)				−0.0406	0.0841	811	−0.4827	0.6294
SST (°C)**				0.1752	0.0538	811	3.2580	0.0012
Lun illum**				−0.1818	0.0695	811	−2.6142	0.0091
Prop day				−0.0524	0.0806	811	−0.6505	0.5155
Prop day: shelf (on)***				−0.6049	0.1013	811	−5.9709	0.0000
No. of Dives	10	1607	4135.057					
(Intercept)***				4.0793	0.1543	1591	26.4449	0.0000
Dist to shore (m)				-5.000^{-6}	2.800^{-6}	1591	−1.8642	0.0625
Dist to shelf break (m)*				6.000^{-6}	3.020^{-6}	1591	1.9903	0.0467
Shelf (on)*				0.2837	0.1131	1591	2.5081	0.0122
Bathymetric depth (m)				−0.0001	3.274^{-5}	1591	−1.5805	0.1142
Prop day***				−0.3785	0.1093	1591	−3.4644	0.0005
Prop day: shelf (on)**				−0.3424	0.1240	1591	−2.7616	0.0058

Notes: SST, sea surface temperature; °C, degree Celsius; Lun illum, fraction of lunar illumination. Other abbreviations and symbols are as in Tables 1–3. Significant covariates from independent LME models (Appendix S3: Table S2) were used to construct full models for stepwise analyses. Bathymetric depth and eddy kinetic energy were included in the full models for mean and max dive depths, but were eliminated during the stepwise procedure.

messages that were appointed to spatial positions did not always commensurate with the resolution of assigned covariates (e.g., dive depths and bathymetry).

Kernel density estimators

*Full dataset (western DPS).—*Grids of UDs based on KDEs (n = 74) for AFSSLs from the wDPS ranged from 182 to 209,844 cells ($\bar{x}$ = 15,608, SD = 34,083), with 1 to 10 monthly grids per individual ranging from October to July (Table 1). Home range polygons were closely aligned with the outlines of CTCRW tracks presented in Figs. 2, 3, whereas core areas were substantially smaller and varied spatially across individuals and time (Fig. 4). Number of grid cells for UDs ranged from 61 to 21,899 ($\bar{x}$ = 3487, SD = 5769) after applying a land mask, data standardization, and defining habitat (Appendix S1). Only one month of data was collected for #61081, so data were not examined at the individual scale for that animal, but they were included in analyses when datasets were pooled across other groups.

Results of IMGAMs varied greatly within and among individuals (Table 6, Appendix S4: Table S1), where k values ranged from 10 to 6130, r^2 values ranged from 0.983 to 0.999, and the percentage deviance explained ranged from 98.9 to

Table 5. Results of a stepwise LME model used to examine maximum dive depths (n = 20,795) from behavior messages obtained for three AFSSLs from the CAI (wDPS) with respect to covariates that were significant for independent LME models. AIC = 14,086.722.

Covariate	Value	SE	DF	*t*-value	*P*
Max Dive Depth					
(Intercept)***	3.2620	0.0915	20,784	35.6694	0.0000
C Season (spring)***	0.2527	0.0222	20,784	11.4067	0.0000
C Season (fall)***	0.1763	0.0195	20,784	9.0483	0.0000
Dist to shore (m)***	4.890^{-5}	2.110^{-6}	20,784	23.1721	0.0000
Dist to shelf break (m)***	-4.240^{-5}	2.180^{-6}	20,784	−19.4416	0.0000
Shelf (on)***	−0.1179	0.0339	20,784	−3.4836	0.0005
EKE (m^2/s^2)***	−14.5901	1.9906	20,784	−7.3295	0.0000
Lun illum***	−0.2261	0.0243	20,784	−9.2998	0.0000
Night***	0.1535	0.0155	20,784	9.9133	0.0000

Notes: EKE, eddy kinetic energy; Night, indicates night dives relative to day dives (dive profiles had a time stamp associated with them); s, second. Other abbreviations and symbols are as in Tables 1–4. Significant covariates from independent LME models (Appendix S3: Table S3) were used to construct the full model for stepwise analysis. Bathymetric depth and slope were included in the full model, but eliminated during the stepwise procedure.

99.9 for 72 of the models. Two IMGAMs had poor model fits (r^2 = 0.470–0.670, deviance explained = 49.6–69.3% for #14751 during November and #34449 during February, respectively). At the population scale, AFSSL density was negatively related to distance to shore, distance to shelf break, and bathymetric slope, and positively related to EKE (Table 6). After calculating $\bar{\beta}$ estimates for each individual, that is, constructing an average of the effects across months, results indicated distance to shore was the only covariate that was consistently significant (-) for all but one individual (#61089; Table 7). A significant negative relationship between density and distance to the shelf break was also evident for five individuals (Table 7). KDEs of seven AFSSLs were related to bathymetric depth, whereby three of the relationships were positive and the remainder were negative. Negative relationships dominated significant findings for bathymetric slope as well (Table 7, Fig. 5a). Negative relationships between KDEs and SSH were observed for two individuals (#14751 and #61088), which predominantly remained near shore. In contrast, positive relationships were observed for #61142, which targeted a large mesoscale feature south of Agattu Island, and #34449, which primarily used Adak Strait. The KDEs of six individuals were related to EKE, five of which were positive relationships. This was consistent with the effect determined by averaging coefficients across all individuals and months (Table 6).

At the regional scale, KDEs were negatively related to distance to shore and shelf break, and bathymetric slope for AFSSLs from both regions (Fig. 6). KDEs of AFSSLs from the WAI were negatively related to bathymetric depth, whereas KDEs of AFSSLs from the CAI had a positive relationship with bathymetric depth and EKE (Fig. 6). This was not surprising given all of the individuals demonstrating a positive relationship with EKE were from the CAI.

At the monthly scale, coefficients were significantly less than zero for all months, indicating a negative relationship between KDEs and distance to shore (Fig. 7). With the exception of January and March, a similar trend was found for distance to shelf break. Curiously, the trend for depth across months appeared to be opposite that of the trend for distance to shelf break (and to some extent shore), indicating that depth did not always covary linearly with distance to the shelf edge. This was evident when AFSSLs traveled through a deep island pass (e.g., Amchitka Pass) from one shelf area to another shelf area or in other areas where the continental shelf is not continuous throughout the Aleutian Arc. KDEs increased with an increase in SSH from late fall to early winter, but then exhibited a negative relationship from late winter into early spring. These results may have coincided with AFSSLs moving further from shore during winter (peak during December) and being exposed to more offshore features, but the SSH field was complex

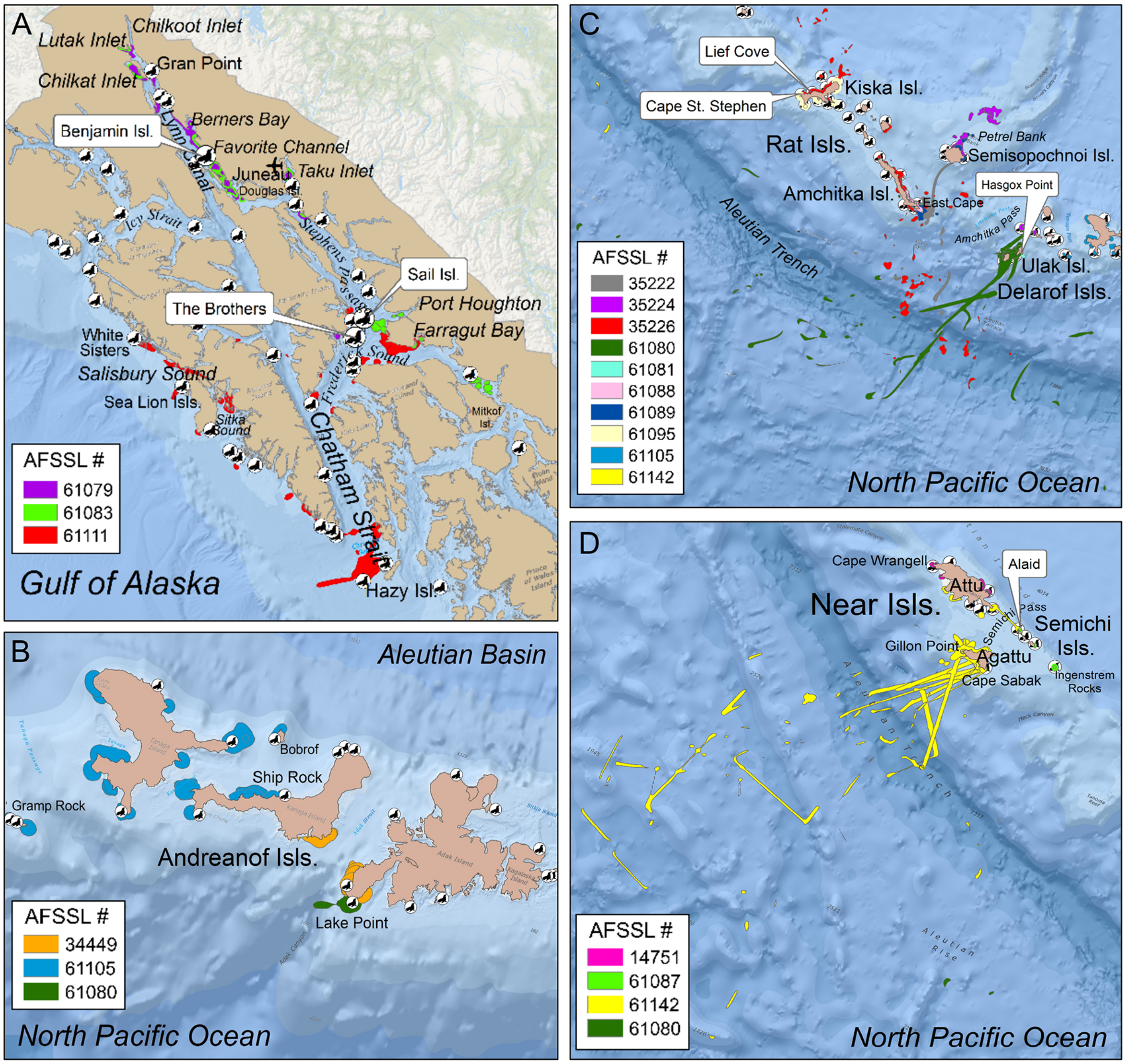

Fig. 4. Pooled core areas (i.e., polygons with 50% isopleths of monthly utilization distributions for full datasets prior to standardization) for AFSSLs in (A) SEAK, (B) the Andreanof Islands, CAI, (C) the Rat and Delarof Islands, CAI, and (D) the Near Islands, WAI.

throughout the study area, changing through time and space. Only positive relationships were observed between KDEs and EKE at the monthly scale (Fig. 7).

Off-shelf dataset (western DPS).—The subset of data corresponding to modeled positions off the continental shelf resulted in 28 KDE UDs ranging from 256 to 207,408 grid cells ($\bar{x}$ = 36,106, SD = 46,432), with 2 to 6 monthly grids for 6 individuals (Table 6) ranging from October to May. The number of grid cells ranged from 145 to 21,119 ($\bar{x}$ = 7435, SD = 7101) after applying a land mask, standardizing the data, and defining habitat.

For the off-shelf KDE UDs, the basis function of IMGAMs could not be increased beyond 50 for one monthly dataset (#35226 during April), resulting in a poor model fit (r^2 = 0.301, percentage deviance explained = 31.7). Otherwise, *k* values ranged from 10 to 5250, r^2 values ranged from

Table 6. Number of significant (Sig) relationships (and direction) for environmental covariates of IMGAMs for 74 full UDs (Appendix S4: Table S1) and 28 off-shelf UDs (Appendix S4: Table S2) constructed for 13 AFSSLs from the wDPS.

Covariate	# Sig IMGAM	+ Relationship	− Relationship	$\bar{\beta}$	SE
Full datasets (*n* = 74)					
Dist to shore (m)*	51	2	49	−0.0004	2.6678^{-5}
Dist to shelf break (m)*	16	5	11	-6.2569^{-5}	1.7238^{-5}
Bathymetric depth (m)	14	5	9	4.7022^{-5}	6.7823^{-5}
Bathymetric slope (°)*	5	1	4	−0.0011	0.0006
SST (°C)	11	4	7	-3.9986^{-6}	7.2793^{-6}
SSH (m)	10	4	6	−0.0455	0.9187
EKE (m^2/s^2)*	8	5	3	8.5515	3.3330
Off-shelf datasets (*n* = 28)					
Dist to shore (m)	9	2	7	-3.6242^{-9}	9.5000^{-8}
Dist to shelf break (m)*	10	0	10	3.5579^{-8}	3.4100^{-8}
Bathymetric depth (m)*	3	3	0	-1.1431^{-7}	5.9400^{-8}
Bathymetric slope (°)	1	1	0	-9.6292^{-8}	5.4900^{-7}
SST (°C)	6	4	2	0.0002	0.0015
SSH (m)*	3	2	1	0.0090	0.0079
EKE (m^2/s^2)*	6	2	4	0.1178	0.1146

Notes: The weighted population mean ($\bar{\beta}$) and weighted SE of IMGAM coefficients pooled across all datasets (i.e., the population) for each environmental covariate are presented for the full and off-shelf datasets. Abbreviations are IMGAM, individual-based monthly generalized additive model; UD, utilization distribution. Asterisks (*) denote significance as indicated by SE values that did not straddle zero. Other abbreviations and units are as in Tables 1–5.

0.982 to 0.999, and the percentage deviance explained ranged from 98.5 to 100.0 for the remaining 27 IMGAMs (Appendix S4: Table S2). Significant coefficients of IMGAMs for off-shelf datasets were similar to those of full datasets, with a few significant covariates gained or lost (Appendix S4: Table S2). At the population scale, KDEs increased as distance to shelf break, SSH, and EKE increased, whereas the opposite occurred for bathymetric depth (Table 6); this was likely owing to limits imposed on bathymetry.

Significant negative relationships between KDEs and distance to shore remained for all but two sea lions (#61142 and #61080) at the individual scale (Table 7). Significant relationships with distance to shelf break emerged for five individuals (#35224, #61089, #61080, #35226, and #35222); all relationships were negative, with the exception of #61080, which had some core areas much further from the shelf edge. Unlike the full datasets, KDEs were not related to slope (with the exception of #61089), likely a result of AFSSLs switching to an epipelagic foraging strategy beyond the shelf break (e.g., epipelagic diving was evident because dives rarely exceeded 200 m for AFSSLs that used deeper waters off-shelf).

For dynamic covariates, a positive relationship between KDEs and SST was retained for #35222 (Fig. 5b) and gained for #35226, whereas a negative relationship emerged for #35224. Opposing relationships for SSH and EKE emerged for #35224 and #35222 (Table 7). Visual inspection of eddy field data indicated #35222 (+ SSH and − EKE) was associated with the rim of a cyclonic feature and the core of an anticyclone, both of which have greater SSH values (Fig. 5b). Additionally, #35224 (− SSH and + EKE) appeared to use the rim of an anticyclonic feature (Fig. 5c), albeit this was not apparent in any IMGAMs (Appendix S4: Table S2). Positive relationships between KDEs and SSH also became apparent for #35226 and #61080, with the latter AFSSL also having a positive relationship with EKE.

At the monthly scale, patterns of significant coefficients for static covariates resembled those of full datasets (Fig. 7). However, a positive relationship between KDEs and distance to shelf break was apparent during October, whereas negative relationships between KDEs and distance to shelf break appeared for two additional months (January and March). In contrast, patterns of significant coefficients for dynamic variables varied more from the patterns of full datasets (Fig. 7).

Table 7. The $\bar{\beta} \pm$ (SE) for environmental covariates from IMGAMs pooled for each wDPS AFSSL across months (mo.) for full and off-shelf (bold) datasets.

AFSSL #	# mo.	Dist shore	Dist shelf break	Depth	Slope	SST	SSH	EKE
35224	6	-4.03^{-4*}	-1.04^{-5}	-1.29^{-4*}	-7.17^{-4}	-4.00^{-6}	0.50	1.02
		(7.10^{-5})	(2.08^{-5})	(8.54^{-5})	(7.58^{-4})	(7.28^{-6})	(1.89)	(8.98)
	5	$\mathbf{-1.37^{-4*}}$	$\mathbf{-1.36^{-4*}}$	$\mathbf{-1.06^{-4*}}$	$\mathbf{-8.45^{-4}}$	$\mathbf{-1.86*}$	$\mathbf{-3.32*}$	$\mathbf{16.82*}$
		$\mathbf{(9.34^{-5})}$	$\mathbf{(2.76^{-5})}$	$\mathbf{(1.02^{-4})}$	$\mathbf{(9.57^{-4})}$	**(1.13)**	**(2.22)**	**(10.32)**
14751	9	-4.21^{-4*}	-1.60^{-4*}	-3.62^{-4}	-4.40^{-3*}	2.81	$-14.93*$	-10.06
		(9.23^{-5})	(7.60^{-5})	(4.49^{-4})	(2.96^{-3})	(2.87)	(11.57)	(24.58)
61087	2	-6.12^{-4*}	-9.23^{-5*}	-9.03^{-4*}	6.19^{-4}	$-3.91*$	5.92	-16.02
		(1.38^{-4})	(7.61^{-5})	(3.44^{-4})	(2.48^{-3})	(2.91)	(7.90)	(39.51)
61142	10	-4.68^{-4*}	1.51^{-5}	1.79^{-5}	-1.25^{-3}	-1.71	$0.43*$	0.70
		(1.09^{-4})	(9.93^{-5})	(2.16^{-4})	(2.48^{-3})	(1.75)	(0.42)	(1.52)
	6	$\mathbf{6.87^{-4*}}$	$\mathbf{-6.81^{-5}}$	$\mathbf{-3.70^{-5}}$	$\mathbf{-7.01^{-4}}$	$\mathbf{-7.64^{-4}}$	**0.16**	**0.76**
		$\mathbf{(2.24^{-4})}$	$\mathbf{(9.24^{-5})}$	$\mathbf{(1.64^{-4})}$	$\mathbf{(1.76^{-3})}$	**(1.00)**	**(0.38)**	**(1.69)**
61089	3	-1.01^{-4}	-1.34^{-5}	2.28^{-4}	3.02^{-3*}	$-2.24*$	0.63	$50.13*$
		(1.41^{-4})	(6.35^{-5})	(2.39^{-4})	(2.36^{-3})	(2.07)	(5.63)	(35.64)
	2	$\mathbf{-9.04^{-6}}$	$\mathbf{-3.30^{-4*}}$	$\mathbf{2.98^{-4*}}$	$\mathbf{2.56^{-3*}}$	**1.45**	$\mathbf{-2.12}$	$\mathbf{-20.54}$
		$\mathbf{(1.58^{-4})}$	$\mathbf{(8.48^{-5})}$	$\mathbf{(2.41^{-4})}$	$\mathbf{(2.33^{-3})}$	**(2.40)**	**(6.56)**	**(38.48)**
61080	6	-1.97^{-4*}	-3.40^{-5}	-1.29^{-4*}	5.44^{-5}	-1.34	-0.23	-12.75
		(1.04^{-4})	(5.54^{-5})	(1.11^{-4})	(1.08^{-3})	(1.67)	(1.75)	(13.34)
	6	$\mathbf{-3.36^{-9}}$	$\mathbf{3.58^{-8*}}$	$\mathbf{-1.14^{-7*}}$	$\mathbf{-9.63^{-8}}$	$\mathbf{2.05^{-4}}$	$\mathbf{8.95^{-3*}}$	$\mathbf{0.12*}$
		$\mathbf{(9.50^{-8})}$	$\mathbf{(3.41^{-8})}$	$\mathbf{(5.94^{-8})}$	$\mathbf{(5.49^{-7})}$	$\mathbf{(1.47^{-3})}$	$\mathbf{(7.91^{-3})}$	**(0.11)**
61095	9	-6.11^{-4*}	-8.04^{-5*}	1.38^{-3*}	-2.95^{-3*}	-0.18	1.51^{-3}	$33.52*$
		(7.88^{-5})	(5.69^{-5})	(2.98^{-4})	(2.61^{-3})	(1.42)	(5.01)	(22.19)
35226	8	-8.94^{-4*}	2.00^{-5}	-2.28^{-5}	-1.41^{-3*}	-0.32	0.52	$7.89*$
		(7.54^{-5})	(4.00^{-5})	(1.14^{-4})	(1.12^{-3})	(0.99)	(1.19)	(5.18)
	6	$\mathbf{-1.36^{-4*}}$	$\mathbf{-2.46^{-4*}}$	$\mathbf{3.26^{-4*}}$	$\mathbf{7.64^{-5}}$	$\mathbf{1.84*}$	$\mathbf{1.88*}$	$\mathbf{-4.14}$
		$\mathbf{(5.23^{-5})}$	$\mathbf{(4.49^{-5})}$	$\mathbf{(1.33^{-4})}$	$\mathbf{(1.33^{-3})}$	**(1.00)**	**(1.22)**	**(6.37)**
34449	4	-3.25^{-4*}	5.65^{-5}	7.31^{-4*}	4.06^{-3}	-0.74	$17.55*$	$46.73*$
		(8.66^{-5})	(7.77^{-5})	(4.31^{-4})	(4.08^{-3})	(2.06)	(5.54)	(28.18)
35222	2	-2.61^{-4*}	3.18^{-6}	-9.58^{-5}	-1.67^{-3*}	$2.52*$	0.06	$-30.84*$
		(8.72^{-5})	(4.68^{-5})	(1.33^{-4})	(1.20^{-3})	(0.95)	(1.86)	(12.97)
	2	$\mathbf{-2.76^{-4*}}$	$\mathbf{-1.49^{-4*}}$	$\mathbf{1.01^{-5}}$	$\mathbf{-8.50^{-4}}$	$\mathbf{1.96*}$	$\mathbf{2.93*}$	$\mathbf{-50.78*}$
		$\mathbf{(9.77^{-5})}$	$\mathbf{(5.02^{-5})}$	$\mathbf{(1.37^{-4})}$	$\mathbf{(1.39^{-3})}$	**(0.95)**	**(2.09)**	**(14.44)**
61088	7	-6.03^{-4*}	-1.37^{-4*}	2.48^{-4*}	-9.45^{-4}	1.06	$-4.07*$	$39.47*$
		(7.44^{-5})	(4.65^{-5})	(1.90^{-4})	(1.62^{-3})	(2.20)	(3.12)	(16.29)
61105	7	-1.66^{-4*}	-5.77^{-5*}	-1.80^{-4*}	4.28^{-4}	$-3.55*$	-2.86	1.39
		(3.34^{-5})	(2.74^{-5})	(1.41^{-4})	(1.35^{-3})	(1.56)	(3.45)	(12.79)

Notes: Abbreviations and units are as in Tables 1–6. Symbols are as in Table 6.

Discussion

To our knowledge, this study provided the longest duration of telemetry data available for AFSSLs and the first winter dataset for AFSSLs in SEAK and western Alaska. Similar to previous studies of AFSSL (Loughlin et al. 1998, Andrews et al. 2002) and other species of lactating sea lions (Thompson et al. 1998, McHuron et al. 2016, Briscoe et al. 2018), habitat use varied considerably within and among individual AFSSLs during this study. Overall, movements and diving behaviors of AFSSLs from SEAK resembled the seasonal distribution of predictable forage fish, whereas individuals from western Alaska utilized a variety of marine ecosystems, providing new insights into the foraging ecology of AFSSLs from those areas.

SEAK AFSSLs (eastern DPS)

During this study, the seasonal changes of inferred foraging locations based on diving behaviors, movements, and core areas of AFSSLs from SEAK bore striking similarities to patterns

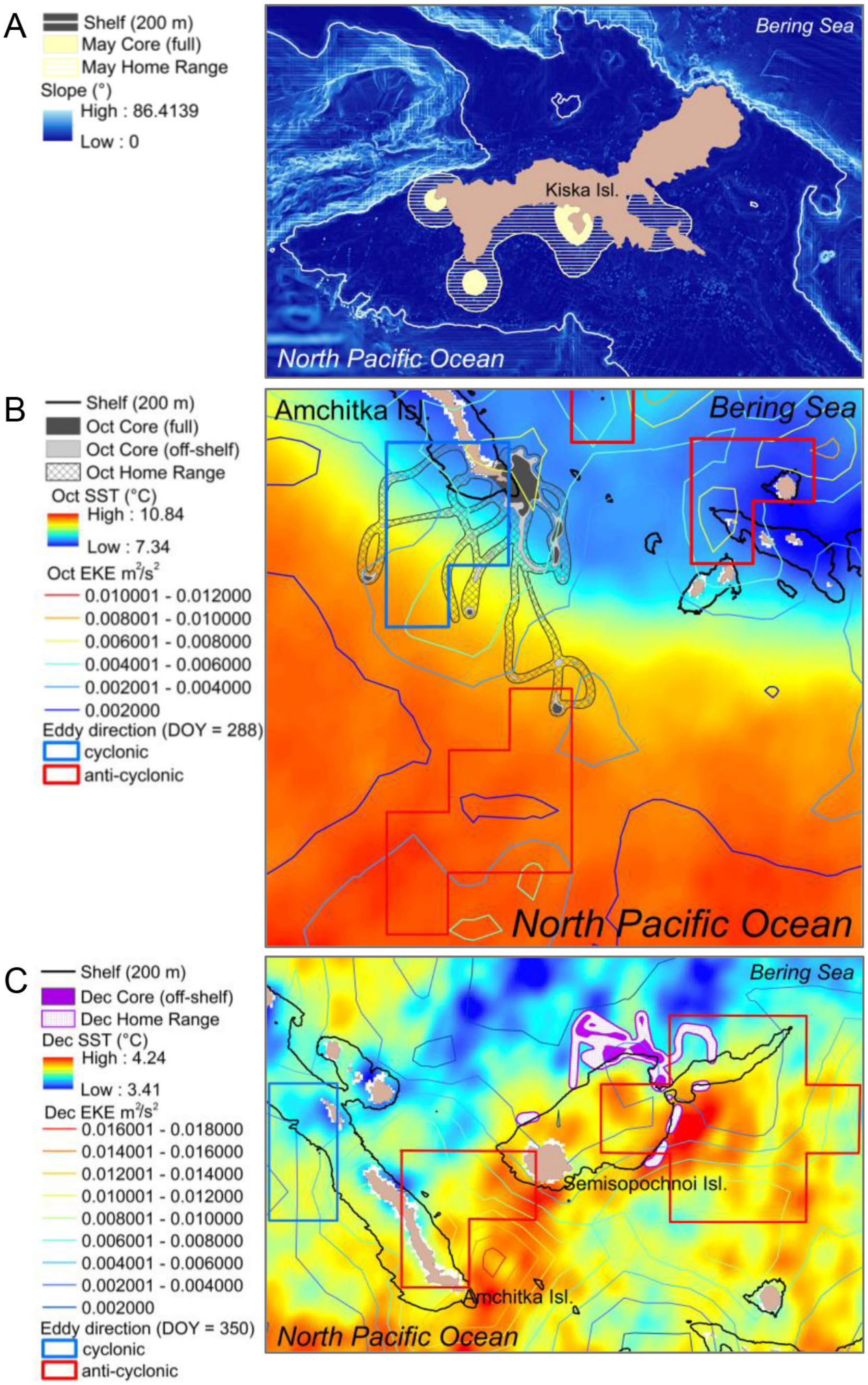

Fig. 5. Examples of monthly core (50% isopleths) and home range (95% isopleths) polygons plotted with respect to select environmental covariates to illustrate significant cases provided in Table 7, including (A) a negative relationship between kernel density estimates (KDEs) and bathymetric slope for the full dataset for AFSSL #61095, (B) relationships between KDEs and sea surface temperature (SST) (+) and eddy kinetic energy (EKE) (−) for the full dataset, and SST (+), sea surface height (SSH) (+), and EKE (−) for the off-shelf dataset for

(Fig. 5. *Continued*)

AFSSL #35222, and (C) relationships between KDEs and SST (−), SSH (−), and EKE (+) for the off-shelf dataset for AFSSL #35224. Months chosen to illustrate examples were cases when the significance (A, B) or coefficient signs (C) of individual-based monthly generalized additive models (IMGAMs) were the same as those provided for the individual as a whole. C is celsius, DOY is day of year, m is meter, and s is second.

reported for SSLs and their prey in the literature (Sigler et al. 2004, 2009, Womble et al. 2005, 2009, Gende and Sigler 2006*a*, *b*, Sigler and Csepp 2007). More specifically, the behaviors of AFSSLs from SEAK during this study appeared to conform to the foraging strategy proposed by Womble et al. (2009) who hypothesized SSLs consume walleye pollock (*Gadus chalcogrammus*) year-round while utilizing areas that allow for efficient predation on seasonal prey items, including (1) Pacific herring (*Clupea pallasii*) aggregations during winter, (2) forage fish spawning aggregations during spring, and (3) migrating Pacific salmon (*Oncorhynchus* spp.) during summer and fall.

Similar to other studies (Andrews et al. 2002, Rehberg et al. 2009), AFSSLs from SEAK dove deeper than AFSSLs from the wDPS. Deeper mean dive depths of SEAK AFSSLs during winter were fairly consistent with the seasonal patterns of mean dive depths reported for tagged juvenile SSLs in SEAK (Sigler et al. 2009) and the movement of adult Pacific herring to deeper depths at wintering grounds (January–February) or spawning beaches (February–March; Carlson 1980). During this study, #61079 used common overwintering areas of Pacific herring in Favorite Channel (Gende and Sigler 2006*a*, *b*) from November to April, primarily around her capture site (i.e., Benjamin Island). The distribution, diet, and prey fields of SSLs in this area have been well studied, and previous researchers have proposed the seasonal use of Benjamin Island by SSLs allows them to locate predictable, energy-rich prey (Gende and Sigler 2006*a*, *b*, Womble and Sigler 2006). In contrast, the two AFSSLs captured in Frederick Sound (#61083 and #6111) presumably targeted overwintering herring sites in that area, but also moved elsewhere possibly because herring are not as predictable in Frederick Sound as they are in Lynn Canal (Womble and Sigler 2006, Sigler and Csepp 2007, Sigler et al. 2009). For example, #61083 used Port Houghton, which is also occupied by walleye pollock (Sigler et al. 2009), whereas #61111 moved to Sitka Sound, which contains one of the largest herring stocks in SEAK (Hebert 2012).

Steller sea lions are less common at Benjamin Island during spring (Gende and Sigler 2006*a*, Womble and Sigler 2006) when the body composition (lipid and protein content) and energy density of herring decreases (Gende and Sigler 2006*a*, Vollenweider et al. 2011) and herring move out of the area (Gende and Sigler 2006*a*, Womble and Sigler 2006). These conditions likely accounted for #61079 and #61083 moving into Berners Bay during April (within a day of each other) before proceeding into northern inlets to probably feed on eulachon (*Thaleichthys pacificus*) spawning runs (Womble et al. 2005, Willson et al. 2006). Sigler et al. (2004) found SSL abundance increased in Berners Bay when prespawning aggregations of eulachon formed during April–May and suggested the eulachon pulse was predictable and likely important to SSLs while experiencing increased energetic demands (e.g., gestation, lactation, and accumulation of fat stores for the breeding season). Following the peak in Berners Bay, large aggregations of SSLs have also been observed at other eulachon spawning sites, including Gran Point and Taku Inlet (Womble 2003, Sigler et al. 2004), which were visited by #61079 (Gran Point) and #61083 (Gran Point and Taku Inlet). The Taku River also has a large Chinook salmon (*O. tshawytscha*) spring run from late April to early July (McPherson et al. 2004, Jones et al. 2010).

The movements of #61079 and #61111 converged during June in Frederick Sound, an important migratory corridor to spawning grounds for *Oncorhynchus* spp., including pink salmon (*O. gorbuscha*; Heard 1991, Womble et al. 2005, 2009). Salmon in this area have been characterized as a high-energy, epipelagic forage species (Womble et al. 2005, 2009, Vollenweider

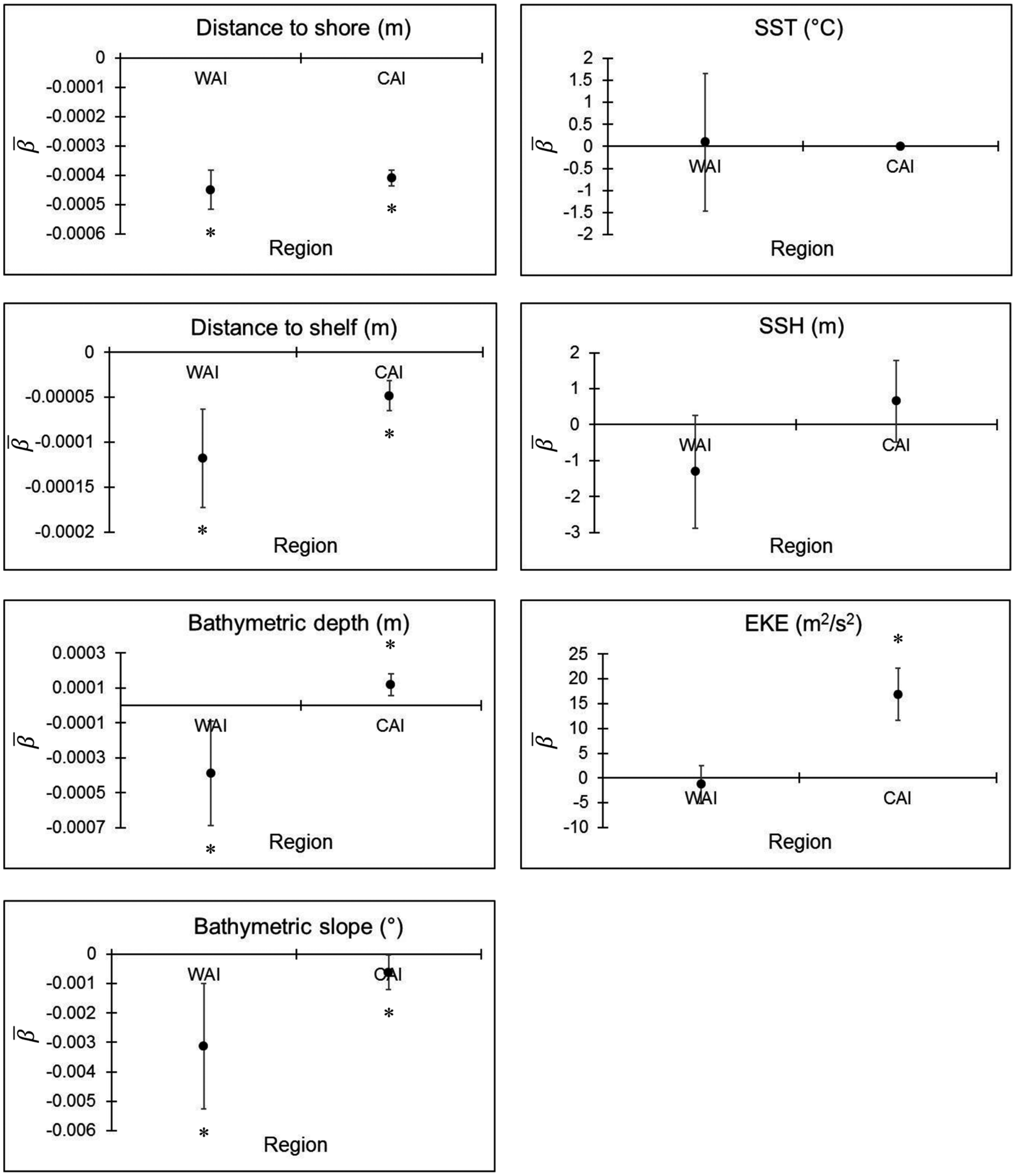

Fig. 6. The weighted population mean ($\bar{\beta}$) ± weighted standard error (SE; bars) of IMGAM coefficients for each environmental covariate pooled across AFSSLs for each region. Asterisks denote significance as indicated by SE values that did not straddle zero.

et al. 2011), which may account for the shallower dive depths observed for AFSSLs during summer.

Western Alaska AFSSLs (western DPS)

Unlike AFSSLs in SEAK, which seemingly targeted predictable prey resources in areas that

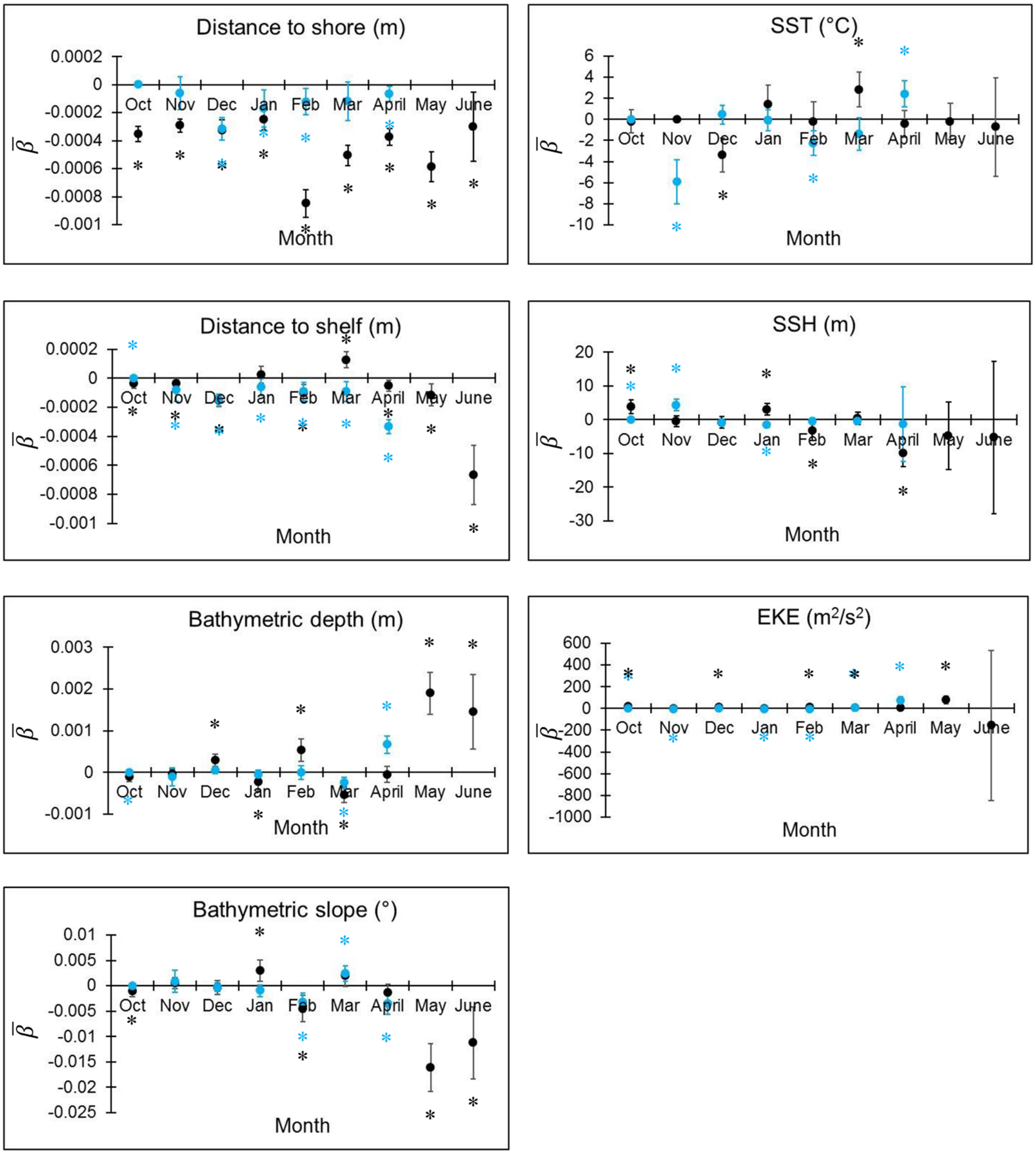

Fig. 7. The $\bar{\beta}$ ± SE of IMGAM coefficients for each environmental covariate pooled across AFSSLs for each month for the full dataset (black symbols) and off-shelf dataset (blue symbols).

have been well studied, paucity of data made it challenging to find analogous associations with prey field distributions in western Alaska. However, relationships between diving behaviors and most static environmental covariates were consistent between the two datasets (i.e., pooled vs. western Alaska), suggesting western AFSSLs may have been targeting predictable prey resources in a similar manner, at least while in shelf waters. Though speculative, this assumption seems sensible as static features may provide a more consistent (and possibly reliable) source of habitat for prey.

For the wDPS, distance to shore was the only predictor variable that consistently influenced the diving behaviors and KDEs of AFSSLs across scales, corroborating findings for juvenile SSLs in the Aleutian Islands (Fadely et al. 2005, Hui et al. 2015). Overall, dive depths increased with distance to shore, whereas frequency of diving and KDEs were greater near shore on the continental shelf. AFSSLs are non-migratory, land-based pinnipeds that return to shore to provision their pups after the breeding season (NRC 2003). Not only is it advantageous for AFSSLs to remain close to shore for this reason, but it enables them to become familiar with their surrounding environment while possibly maximizing their foraging opportunities and energy intake (Orians and Pearson 1979, Womble et al. 2009). Although AFSSLs exhibit some site fidelity to haulout sites (Trites et al. 2006), some individuals are multiple central place foragers that seemingly alter their behavior depending on prey availability near a given haulout site (Raum-Suryan et al. 2004). Assuming this is true, inter-haulout movements conducted by SSLs allow them to maintain a minimum distance to shore while foraging.

Although diet studies indicate AFSSLs and juveniles consume a variety of species, they do appear to exhibit fidelity to prey that are seasonally predictable in shelf waters (Sinclair and Zeppelin 2002, Sinclair et al. 2013). Two decades (1990–2009) of data based on all prey remains found in SSL fecal samples in western Alaska (west of Samalga Pass) indicated Atka mackerel (*Pleurogrammus monopterygius*) dominated the diet year-round, but during more recent years, the frequency of occurrence of some primary prey species differed slightly between seasons (Sinclair et al. 2013). The diet was more diverse during winter when Pacific cod (*Gadus macrocephalus*), Irish lords (*Hemilepidotus* spp.), walleye pollock, rockfishes (*Sebastes* spp.), snailfishes (Liparididae), and some other species were more prominent, whereas Atka mackerel and salmon were more prominent in the diet during summer (Sinclair et al. 2013). Tollit et al. (2017) used DNA methods to detect additional species consumed by SSLs during the non-breeding season in western Alaska and confirmed that Atka mackerel dominated the diet, but Pacific cod, smooth lumpsucker (*Aptocyclus ventricosus*), and cephalopod species were important prey. Stable isotope values in vibrissae collected from SSL pups (used as an indicator of pregnant AFSSL diets during winter) indicated AFSSLs from western Alaska also relied on squid, which are typically underrepresented in scat analyses (Scherer et al. 2015). Combined, these studies provide a more comprehensive understanding of SSL diet, which allowed us to interpret some of the patterns in our data for AFSSLs.

The distributions of core areas often were associated with SSL sites, but also overlapped some areas used by other age classes of SSLs (Lander et al. 2009, 2011*a*, *b*, Himes Boor and Small 2012) and some Atka mackerel nesting sites (Lauth et al. 2007*b*). In Alaska, Atka mackerel are patchily distributed and occur in water depths ranging from 70 to 200 m, but they enter shallow waters near shore during the breeding/brooding season, which can last from June to January (McDermott and Lowe 1997, Lowe et al. 1998, Lauth et al. 2007*a*, McDermott et al. 2016). Thus, Atka mackerel may be predictable prey items for AFSSLs during this time (Cooper and McDermott 2011) until they move back into deeper waters and are less accessible (Fritz et al. 2019). The timing of longer, off-shelf trips conducted by some AFSSLs in late fall and winter during this study may have coincided with the timing of Atka mackerel seasonal movements.

Some core areas of AFSSLs, notably those in northern areas of the Petrel Bank shelf break, also occurred in areas known to support concentrations of Pacific cod during the spawning season, which occurs from February to April (Neidetcher et al. 2014). Otherwise, Pacific cod are most abundant on the continental shelf and tend to exhibit site fidelity (Bakkala 1984, Neidetcher et al. 2014, Rand et al. 2014), possibly rendering them predictable prey for AFSSLs as well. During this time of year, smooth lumpsuckers also migrate from deep waters to nearshore areas to spawn at depths <10 m (Mecklenburg et al. 2002, Zhukova et al. 2018), which makes them accessible to AFSSLs in shallow waters and may account for the limited variation in diving behaviors observed across seasons. Although our results were inconsistent with studies that indicated maximum dive depths of wDPS AFSSLs during winter were greater than during summer (Merrick et al. 1994, Merrick and Loughlin 1997), it is important to emphasize that seasons were not defined consistently across studies. A two-season approach (winter vs. summer) produced results more closely aligned with past studies (i.e., Appendix S3: Table S2).

Similar to AFSSLs tagged during the summer breeding season in the Kuril Islands, Russia (Loughlin et al. 1998, Waite et al. 2012), and SEAK (Rehberg et al. 2009), most diving of AFSSLs occurred during night regardless of their distribution. However, mean dive depths of AFSSLs were only deeper during night than during the day when they were in waters over the continental shelf. The spatially explicit diving behaviors inferred for three AFSSLs coupled with the interaction effects (proportion of daylight*on/off shelf) observed for mean dive depths of AFSSLs from the wDPS indicated they were likely feeding on a combination of benthic prey species and species that exhibit reverse diel vertical migration (DVM), or type II DVM (nocturnal descent; Neilson and Perry 1990) while in shelf waters. For example, yellow Irish lord (*H. jordani*) primarily occupy benthic habitat (Reuter and Tenbrink 2008, Tenbrink and Buckley 2013), but Atka mackerel, Pacific cod, and smooth lumpsucker display both benthic and pelagic behaviors (Nichol and Somerton 2002, Orlov and Tokranov 2008, Nichol et al. 2013). Atka mackerel perform surface-directed vertical movements during the day (most likely to feed on zooplankton) and minimal, if any, vertical migration from the seafloor during night (Nichol and Somerton 2002, Rand and Lowe 2011). Pacific cod are also benthic dwellers, but their foraging patterns can vary among individuals, habitats, locations, and seasons (Nichol et al. 2007, 2013).

An interaction effect was not observed for diving behaviors during different lunar fraction conditions while on/off the shelf. Furthermore, inclusion of SEAK AFSSLs in analyses absolved any relationships between diving behaviors and lunar fraction. Otherwise, maximum dive depths were negatively related to lunar fraction for wDPS AFSSLs and this was true even if analyses were confined to nocturnal data. These results were inconsistent with those found for other pinniped species thought to target prey associated with the deep scattering layer (Horning and Trillmich 1999, Ream et al. 2005, Sterling et al. 2014), but consistent with findings for juvenile SSLs from the CAI (Lander et al. 2011*a*), possibly due to SSLs foraging more on larger prey species as opposed to mesopelagic prey (K. Luxa et al., *public communications*. https://static1.squarespace.com/static/596e8ac529687ff6231cda81/t/5c48f20288251b738e022a00/1548284448641/2019_AMSS_abstractbook.pdf).

Bathymetry, substrate, and prey availability may influence the habitat use of benthic predators (Bjørge 2002). Previous studies indicated the diving behaviors and distributions of SSLs (primarily juveniles) were associated with bathymetry or bathymetric features such as seamounts and submarine ridges in Alaska (Merrick 1995, Fadely et al. 2005, Lander et al. 2011*b*). During this study, however, diving behaviors were not associated with bathymetric depth in full models and relationships between KDEs and bathymetry varied across scales. Lack of significance for diving behaviors may have been due to correlation between bathymetry and other covariates, which subsequently provided better model fits in LME analyses.

Although diving behaviors were not related to bathymetric slope, KDEs generally displayed a negative relationship with slope across scales. This was unexpected given various fish species appear to prefer physically complex habitats or high relief substrate (Rooper and Boldt 2005, Lauth et al. 2007*b*), but consistent with findings of Lander et al. (2011*a*), who found the majority of tagged juvenile SSL locations occurred in areas defined as flats. Similarly, Gregr and Trites (2008) found a greater number of SSL observations at sea occurred in areas of lower slope. They also found SSL observations increased as sighting platforms approached depths ranging from 150 to 200 m, which was consistent with the inverse relationships we found between KDEs and distance from the shelf break. It was difficult to tease apart some of our results given the complexity of the environment and some of the UDs, but perhaps the high use of low relief areas on the continental shelf closer to the shelf break outweighed the use of other areas by AFSSLs. Recently, Bryan et al. (2018) conducted optimal surveys of untrawlable prey fields during summer around SSL sites in the WAI and CAI, including some of the core areas presented herein. They found greater densities of some species (Atka mackerel, Irish lords, greenlings, and ronquils) were associated with rockier terrain, but unconsolidated substrate was the most common habitat encountered during surveys. For this study, the spatial resolution of the slope data was greater than the AFSSL UDs; thus, if AFSSL were targeting fish associated with high relief features, this could have been undetected in our data if those features were patchily distributed (or clumped) in broader, low relief areas. Moreover, slope may not be an important indicator of substrate type (Rooper and Zimmermann 2007), the ultimate habitat of prey.

Contrary to tagged juvenile SSLs (NMFS 2014), AFSSLs used off-shelf areas more frequently. During late fall and winter months, three AFSSLs from our study entered off-shelf waters in the Bering Sea Basin, whereas four AFSSLs made longer excursions into deep pelagic waters of the North Pacific Ocean. Diel diving patterns displayed by AFSSLs, coupled with aforementioned SSL diet studies, a concurrent localized prey study (McDermott et al. 2014), and past studies describing the distributions and behaviors of prey species (Favorite 1969, Myers et al. 2007) suggest AFSSLs were likely foraging on a combination of pelagic species (e.g., rockfishes, walleye pollock, salmonids, cephalopods, and possibly Myctophidae) undergoing type I DVM (nocturnal ascent) in the water column. Although adult walleye pollock tend to occupy benthic habitat (continental shelf, break, and slope), they also occur in pelagic waters of the Aleutian/Bering Sea Basins and North Pacific Ocean (Bakkala 1993, Bacheler et al. 2012) and there have been some accounts of adults displaying type I DVM elsewhere (Miyashita et al. 2004, Adams et al. 2007, 2009). Some salmon spp. in the open waters of the Bering Sea and North Pacific Ocean also occur at deeper depths during the day and near the surface at night (Ogura and Ishida 1992, Walker et al. 2007). Additionally, pelagic squid (Gonatidae) and Myctophidae (e.g., *Stenobrachius leucopsarus*) vertically migrate from deeper depths into the epipelagic zone during night (Watanabe et al. 1999, 2006).

Overall, relationships regarding diving behaviors and KDEs of AFSSLs relative to dynamic environmental covariates were not as straightforward as those observed for static covariates. Mean and maximum dive depths were positively related to SST only, whereas no relationships were observed between diving behaviors and SSH or EKE. However, KDEs of AFSSLs varied with these dynamic covariates across spatial and temporal scales. Spatial variation in SST and altimetry data can be indicative of productive frontal features or mesoscale features such as eddies (Paluszkiewicz and Niebauer 1984, Okkonen et al. 2001, Chelton et al. 2007, 2011, Gregr and Trites 2008), which may concentrate prey for marine mammals, including SSLs (Orlov 2003, Fadely et al. 2005, Ream et al. 2005, Gregr and Trites 2008, Lander et al. 2010, Nordstrom et al. 2013, Pelland et al. 2014, Sterling et al. 2014). Relationships with altimetry data should be interpreted with caution for nearshore individuals that made small-scale movements because results were based on data extracted from a few grid cells. Relationships for AFSSLs that moved considerable distances, however, generally indicated KDEs varied in response to SSH and EKE.

Visual inspection of AFSSL UDs relative to altimetry products and OW imagery revealed there were many features present in the areas of most AFSSL tracks associated with Alaskan Currents. Eddies that originate in the Gulf of Alaska often become embedded in the Alaskan Stream, where their trajectories propagate westward along the northern slope of the Aleutian Trench to the CAI (Crawford et al. 2000, Ladd et al. 2007). Drifter and altimetry data (i.e., amplitude and EKE) have signified eddies in the Alaskan Stream south of Amchitka Pass and within Amchitka Pass (Okkonen 1996, Stabeno et al. 1999, Cheng et al. 2014). These features likely influenced the distributions of AFSSLs directly while off-shelf (e.g., #35222, #35224, and possibly #61080), or indirectly while on the shelf (e.g., #34449) via cross-shelf exchange of heat and nutrients (Ueno et al. 2008) influencing the food web dynamics in that area.

Strong inflow through Amchitka Pass can impact the Aleutian North Slope Current and the formation of eddies in the Bering Sea (Maslowski et al. 2014). Sea surface height variability in this area of the CAI is likely a result of flowtopography interactions between eddies, currents, and the slopes of Bowers Ridge (Ezer and Oey 2013). The distribution patterns of #35224 were seemingly influenced by these processes, as she appeared to forage near a small, anticyclonic eddy off Semisopochnoi Island until that feature moved northeast. Though SSH or EKE were not significant covariates for any IMGAMs during that time for #35224, offshore data pooled across months indicated a combination of covariates (− SST, − SSH, and + EKE) consistent with waters adjacent to an anticyclonic, warm-core ring.

Despite the apparent use of mesoscale features by some AFSSLs, scales of measurement (be it for the telemetry or oceanographic data) did not always capture those behaviors statistically. For this reason, it was necessary to plot the data over various scales to aide with data interpretation. For example, #61142 appeared to visit a large, productive, westward moving anticyclonic eddy south of the WAI repeatedly until March, which was evident in altimetry data (Fadely and Lander 2012). From a qualitative standpoint, it also appeared AFSSLs were using various forms of edge habitat, whether in the form of a thermal front, the continental shelf, or a mesoscale feature. Hence, further investigation of AFSSL behaviors and distributions with respect to SST gradients or distances to those features may be informative. For example, Sterling et al. (2014) found adult female northern fur seals (*Callorhinus ursinus*) changed from a transit state to a resident state when near eddy edges in the Gulf of Alaska and California Current.

Other biases associated with the resolution of our environmental data products may have also influenced our results. For example, smaller eddies (i.e., of similar size to the spatial resolution of the altimetry data) possibly went undetected in our OW investigations (Cheng et al. 2014). Additionally, bathymetry has been precisely mapped in many areas of Alaska (Zimmermann and Benson 2013, Zimmermann et al. 2013), but much of it has been modeled (S. Lewis, *personal communication*). Cloud cover also likely impacted SST data, substantially reducing data availability and our model input sample sizes. Lastly, discrepancies in results for dynamic covariates across data groupings may have been due to the greater spatial resolution of remote sensing data coupled with the variable spatial dispersion of the UDs (e.g., some AFSSLs had a greater number of locations spread across a larger geographic area).

Single model inference with GAMs for the KDE analyses allowed us to account for spatial autocorrelation and process large, complex datasets that required a substantial amount of memory and computing time in a standardized fashion. The disadvantage of this approach, however, was that the GAMs were sensitive to sample sizes and the basis size (k) chosen for larger UDs, which required hand-tuning and supervised model checking. Although the mgcv package allowed fitting of these large spatial models in a straightforward and relatively fast way (as opposed to Markov chain Monte Carlo), future studies may benefit from a more black box model for the spatial component.

CONCLUSIONS

Multi-scale analyses provide a greater understanding of habitat use and are helpful for assessing informative scales needed for ecological interpretation and prediction models (Wiens 1989, Acevedo-Gutiérrez 2009, Mayor et al. 2009, McGarigal et al. 2016). For this study, comparisons of foraging behaviors of AFSSLs over time and space revealed pronounced individual variability within overall broader patterns. Diving behaviors varied seasonally and differed between stocks, though most relationships between diving behaviors and static environmental features were consistent between stocks. Within the wDPS, the spatial habitat use of AFSSLs was influenced by some static features (i.e., shore, shelf, and slope) for the population as a whole. Trends for these predictor variables remained similar at the regional scale, and to some extent the monthly scale (shore and shelf), but started to vary at individual scales (both within and among individuals). Given these patterns in the data, it seems reasonable to assume that individual variation in habitat use of these static covariates can be incorporated into predictive models for making population inference for conservation purposes (Wilson et al. 2018). In contrast, habitat associations with dynamic covariates were more scale-dependent and managers should exercise caution when considering dynamic features as important habitat for SSLs at population scales. Rather, analyses should be adjusted to appropriate spatial and seasonal scales (Wilson et al. 2018).

The dynamic features of marine ecosystems (e.g., currents, SST, and eddies) can be challenging to managers when assessing important habitat for species conservation because they encompass ambiguous boundaries that can rapidly fluctuate (Jones 2002, Game et al. 2009, De Santo 2013). The intermittent use of only some dynamic features by some AFSSLs may reflect the fact that these habitat features are by their nature ephemeral, and may not consistently provide enhanced foraging opportunities. Many dynamic processes are persistent or interconnected with static features, however, which can be included in traditional, spatially fixed protected areas (Hyrenbach et al. 2000, Game et al. 2009). Further investigation of the interaction of static and dynamic features and how they are situated relative to designated Steller sea lion critical habitat will be key to understanding the habitat needs of AFSSLs.

ACKNOWLEDGMENTS

We thank Alexi Altukhov, Vladimir Burkanov, Van Helker, Carey Kuhn, and Katie Sweeney of the Alaska Fisheries Science Center (AFSC) for all of their assistance with fieldwork. We also thank Marty Haulena of the Vancouver Aquarium, Kimberlee Beckmen, Aaron Christ, Tom Gage, Lauri Jemison, Justin Jenniges, Mandy Keogh, Sara Longson, Dennis McAllister, Mike Rehberg, and Greg Snedgen of the Alaska Department of Fish and Game (ADF&G), Russ Andrews, Stephanie Kennedy, Marianne Lian, and Lorrie Rea of the University of Alaska Fairbanks, Florence Johnson, Gordon Garcia, and Brad Weinlaeder of the Ted Stevens Marine Research Institute, Joe Gaydos of SeaDoc Society, Kim Goetz, Patrick Robinson, Luis Hückstädt, and Yan Tremblay of the University of California at Santa Cruz, Jason Roberts of Duke University, and the crews of the *M/V NORSEMAN* and *F/T SEAFISHER*. This work was supported by the National Marine Fisheries Service and National Oceanic and Atmospheric Administration Cooperative Agreement NA08NMF 4390544 to the ADF&G SSL Project. Additionally, this research was performed while Noel Pelland held an NRC Research Associateship award at the AFSC. Jim Lee, Katie Luxa, and Kim Rand (AFSC) along with two anonymous reviewers provided helpful comments on the manuscript. From the AFSC, Rebecca White provided assistance with graphics, Jan Benson and Steve Lewis provided GIS support, and Josh London provided some code. All research was conducted under the authority of MMPA/ESA Permits 14326 and 18528, IACUC Protocol Nos. A/NW-2010-4 and A/NW-2013-2, and ACUC Protocol No. 2010-14R 09-28. The use of trade, product, or firm names is for descriptive purposes only and does not imply endorsement by the U.S. Government. The findings and conclusions in the paper are those of the authors and do not necessarily represent the views of the National Marine Fisheries Service.

GlobColour data (http://globcolour.info) used in this study have been developed, validated, and distributed by ACRI-ST, France. The Group for High Resolution Sea Surface Temperature (GHRSST) Multi-scale Ultra-high Resolution (MUR) SST data were obtained from the NASA EOSDIS Physical Oceanography Distributed Active Archive Center (PO.DAAC) at the Jet Propulsion Laboratory, Pasadena, CA (https://doi.org/10.5067/ghgmr-4fj01). The Ssalto/Duacs altimeter products were produced and distributed by the Copernicus Marine and Environment Monitoring Service (CMEMS) (http://www.marine.copernicus.eu).

LITERATURE CITED

Acevedo-Gutiérrez A. 2009. Habitat use. Pages 524–528 *in* W. F. Perrin, B. Würsig, and J. G. M. Thewissen, editors. Encylopedia of marine mammals. Second edition. Academic Press, San Diego, California, USA.

Adams, C. F., R. J. Foy, J. J. Kelley, and K. O. Coyle. 2009. Seasonal changes in the diel vertical migration of walleye pollock (*Theragra chalcogramma*) in the northern Gulf of Alaska. Environmental Biology of Fishes 86:297–305.

Adams, C. F., A. I. Pinchuk, and K. O. Coyle. 2007. Seasonal changes in the diet composition and prey selection of walleye pollock (*Theragra chalcogramma*) in the northern Gulf of Alaska. Fisheries Research 84:378–389.

Altukhov, A., et al. 2015. Age specific survival rates of Steller sea lions at rookeries with divergent population trends in the Russian Far East. PLOS ONE 10: e0127292.

Andrews, R. D., D. G. Calkins, R. W. Davis, B. L. Norcross, K. Peijnenberg, and A. W. Trites. 2002. Foraging behavior and energetics of adult female Steller sea lions. Pages 19–22 *in* D. DeMaster and S. Atkinson, editors. Steller sea lion decline: is it food II. AK-SG-02-02. University of Alaska Sea Grant, Fairbanks, Alaska, USA.

Bacheler, N. M., L. Ciannelli, K. M. Bailey, and V. Bartolino. 2012. Do walleye pollock exhibit flexibility in where or when they spawn based on variability in water temperature? Deep-Sea Research II 65–70:208–216.

Bakkala, R. G. 1984. Pacific cod in the eastern Bering Sea. International North Pacific Fisheries Commission 42:157–179.

Bakkala, R. G. 1993. Structure and historical changes in the groundfish complex of the eastern Bering Sea. NOAA Technical Report, vol. 114. U.S. Department of Commerce, National Technical Information Service, Springfield, Virginia, USA.

Bjørge, A. 2002. How persistent are marine mammal habitats in an ocean of variability? Pages 63–91 *in* P. G. H. Evans and J. A. Raga, editors. Marine mammals: biology and conservation. Springer, Boston, Massachusetts, USA.

Block, W. M., and L. A. Brennan. 1993. The habitat concept in ornithology: theory and applications. Pages 35–91 *in* D. M. Power, editor. Current ornithology. Volume 11. Springer-Verlag, New York, New York, USA.

Braham, H. W., R. D. Everitt, and D. G. Rugh. 1980. Northern sea lion decline in the eastern Aleutian Islands. Journal of Wildlife Management 44:25–33.

Briscoe, D. K., et al. 2018. Characterizing habitat suitability for a central-place forager in a dynamic marine environment. Ecology and Evolution 8:2788–2801.

Bryan, D. R., M. Levine and S. McDermott. 2018. Results of the 2016 and 2017 Central and Western Aleutian Islands underwater camera survey of Steller sea lion prey fields. NOAA Technical Memorandum, NMFS–AFSC–381. National Marine Fisheries Service, Alaska Fisheries Science Center, Seattle, Washington, USA.

Caballero, A., A. Pascual, G. Dibarboure, and M. Espino. 2008. Sea level and eddy kinetic energy variability in the Bay of Biscay, inferred from satellite altimeter data. Journal of Marine Systems 72:116–134.

Carlson, H. R. 1980. Seasonal distribution and environment of Pacific herring near Auke Bay, Lynn Canal, Southeastern Alaska. Transactions of the American Fisheries Society 109:71–78.

Chelton, D. B., M. G. Schlax, and R. M. Samelson. 2011. Global observations of nonlinear mesoscale eddies. Progress in Oceanography 91:167–216.

Chelton, D. B., M. G. Schlax, R. M. Samelson, and R. A. de Szoeke. 2007. Global observations of large oceanic eddies. Geophysical Research Letters 34: L15606.

Cheng, Y.-H., C.-R. Ho, Q. Zheng, and N. Kuo. 2014. Statistical characteristics of mesoscale eddies in the North Pacific derived from satellite altimetry. Remote Sensing 6:5164–5183.

Cooper, D., and S. McDermott. 2011. Seasonal, small-scale distribution of Atka mackerel in the Aleutian Islands, Alaska, with respect to reproduction. Marine and Coastal Fisheries: Dynamics, Management, and Ecosystem Science 3:10–20.

Crawford, W. R., J. Y. Cherniawsky, and M. G. G. Foreman. 2000. Multi-year meanders and eddies in the Alaskan Stream as observed by TOPEX/Poseidon altimeter. Geophysical Research Letters 27:1025–1028.

De Santo, E. M. 2013. Missing marine protected area (MPA) targets: How the push for quantity over quality undermines sustainability and social justice. Journal of Environmental Management 124:137–146.

Ezer, T., and L. Oey. 2013. On the dynamics of strait flows: an ocean model study of the Aleutian passages and the Bering Strait. Ocean Dynamics 63:243–263.

Fadely, B., and M. Lander. 2012. Satellite tracking of adult female Steller sea lions in the Western-Central Aleutian Islands reveals diverse foraging behaviors. Alaska Fisheries Science Center, Seattle, Washington, USA. http://www.afsc.noaa.gov/quarterly/ond2012/divrptsNMML1.htm

Fadely, B. S., B. W. Robson, J. T. Sterling, A. Greig, and K. A. Call. 2005. Immature Steller sea lion (*Eumetopias jubatus*) dive activity in relation to habitat features of the eastern Aleutian Islands. Fisheries Oceanography 14:243–258.

Favorite, F. 1969. Fishery oceanography V: ocean circulation and distribution of sockeye salmon. Commercial Fisheries Review 31:85–89.

Fay, G., and A. Punt. 2006. Modeling spatial dynamics of Steller sea lions (*Eumetopias jubatus*) using maximum likelihood and Bayesian methods: evaluating causes for population decline. Pages 405–434 *in* A. W. Trites, S. K. Atkinson, D. P. DeMaster, L. W. Fritz, T. S. Gelatt, L. D. Rea, and K. M. Wynne, editors. Sea lions of the world. Proceedings of the Lowell Wakefield Fisheries Symposium, Anchorage, Alaska, September 30–October 3, 2004. Alaska Sea Grant College Program, AK–SG–06–01. Fairbanks, Alaska, USA.

Fritz, L., B. Brost, E. Laman, K. Luxa, K. Sweeney, J. Thomason, D. Tollit, W. Walker, and T. Zeppelin. 2019. A re-examination of the relationship between Steller sea lion diet and population trend using data from the Aleutian Islands. Canadian Journal of Zoology 97:1137–1155.

Fritz, L. W., R. Towell, T. S. Gelatt, D. S. Johnson, and T. R. Loughlin. 2014. Recent increases in survival of western Steller sea lions in Alaska and implications for recovery. Endangered Species Research 26:13–24.

Game, E. T., H. S. Grantham, A. J. Hobday, R. L. Pressey, A. T. Lombard, L. E. Beckley, K. Gjerde, R.

Bustamante, H. P. Possingham, and A. J. Richardson. 2009. Pelagic protected areas: the missing dimension in ocean conservation. Trends in Ecology and Evolution 24:360–369.

Gende, S. M., and M. F. Sigler. 2006*a*. Persistence of forage fish 'hot spots' and its association with foraging Steller sea lions (*Eumetopias jubatus*) in southeast Alaska. Deep-Sea Research Part II 53:432–441.

Gende, S. M., and M. F. Sigler. 2006*b*. Predictability of prey available to Steller sea lions in Southeastern Alaska. Pages 69–81 *in* A. W. Trites, S. K. Atkinson, D. P. DeMaster, L. W. Fritz, T. S. Gelatt, L. D. Rea, and K. M. Wynne editors. Sea lions of the world. Proceedings of the Lowell Wakefield Fisheries Symposium, Anchorage, Alaska, September 30–October 3, 2004. Alaska Sea Grant College Program, AK–SG–06–01. Fairbanks, Alaska, USA.

Gregr, E. J., and A. W. Trites. 2008. A novel presence-only validation technique for improved Steller sea lion *Eumetopias jubatus* critical habitat descriptions. Marine Ecology Progress Series 365:247–261.

Hall, L. S., P. R. Krausman, and M. L. Morrison. 1997. The habitat concept and a plea for standard terminology. Wildlife Society Bulletin 25:173–182.

Haulena, M. 2007. Otariid seals. Pages 469–478 *in* G. West, D. Heard, and N. Caulkett, editors. Zoo animal and wildlife immobilization and anesthesia. Blackwell Publishing, Ames, Iowa, USA.

Haulena, M. 2014. Otariid seals. Pages 661–672 *in* G. West, D. Heard, and N. Caulkett, editors. Zoo animal and wildlife immobilization and anesthesia. Second edition. John Wiley & Sons Inc, Ames, Iowa, USA.

Heard, W. R. 1991. Life history of pink salmon *Oncorhynchus gorbuscha*. Pages 119–230 *in* C. Groot and L. Margolis, editors. Pacific salmon life histories. University of British Columbia Press, Vancouver, Canada.

Heath, R. B., D. G. Calkins, D. McAllister, W. Taylor, and T. Spraker. 1996. Telazol and isoflurane field anesthesia in free-ranging Steller's sea lions (*Eumetopias jubatus*). Journal of Zoo and Wildlife Medicine 27:35–43.

Hebert, K. 2012. Southeast Alaska 2010 herring stock assessment surveys. Fishery Data Series No. 12–46. Alaska Department of Fish and Game, Divisions of Sport Fish and Commercial Fisheries, Anchorage, Alaska, USA.

Henson, S. A., and A. C. Thomas. 2007. A census of oceanic anticyclonic eddies in the Gulf of Alaska. Deep Sea Research I 55:163–176.

Himes Boor, G. K., and R. J. Small. 2012. Steller sea lion spatial-use patterns derived from a Bayesian model of opportunistic observations. Marine Mammal Science 28:E375–E403.

Holmes, E. E., L. W. Fritz, A. E. York, and K. Sweeney. 2007. Age-structured modeling reveals long-term declines in the natality of western Steller sea lions. Ecological Applications 17:2214–2232.

Holmes, E. E., and A. E. York. 2003. Using age structure to detect impacts on threatened populations: a case study with Steller sea lions. Conservation Biology 17:1794–1806.

Hooker, S. K., A. Cañadas, K. D. Hyrenbach, C. Corrigan, J. J. Polovina, and R. R. Reeves. 2011. Making protected area networks effective for marine top predators. Endangered Species Research 13:203–218.

Horning, M., and J. E. Mellish. 2012. Predation on an upper trophic marine predator, the Steller sea lion: evaluating high juvenile mortality in a density dependent conceptual framework. PLOS ONE 7: e30173.

Horning, M., and F. Trillmich. 1999. Lunar cycles in diel prey migrations exert a stronger effect on the diving of juveniles than adult Galápagos fur seals. Proceedings of the Royal Society of London B 266:1127–1132.

Hui, T. C. Y., R. Gryba, E. J. Gregr, and A. W. Trites. 2015. Assessment of competition between fisheries and Steller sea lions in Alaska based on estimated prey biomass, fisheries removals and predator foraging behavior. PLOS ONE 10: e0123786.

Hyrenbach, K. D., F. A. Forney, and P. K. Dayton. 2000. Viewpoint: marine protected areas and ocean basin management. Aquatic Conservation: Marine and Freshwater Ecosystems 10:437–458.

Jessopp, M., M. Cronin, and T. Hart. 2013. Habitat-mediated dive behavior in free-ranging grey seals. PLOS ONE 8:e63720.

Johnson, D. H. 1980. The comparison of usage and availability measurements for evaluating resource preference. Ecology 61:65–71.

Jones, P. J. S. 2002. Marine protected area strategies: issues, divergences and the search for middle ground. Review in Fish Biology and Fisheries 11:197–216.

Jones, E. L. III, S. A. McPherson, D. J. Reed, and I. M. Boyce. 2010. Spawning abundance of Chinook salmon in the Taku River from 1999 to 2007. Fishery Data Series No. 10–70. Alaska Department of Fish and Game, Divisions of Sport Fish and Commercial Fisheries, Anchorage, Alaska, USA.

Kalarus, K., and P. Nowicki. 2017. Resource use by the dryad butterfly is scale-dependent. Population Ecology 59:179–187.

Ladd, C., C. W. Mordy, N. B. Kachel, and P. J. Stabeno. 2007. Northern Gulf of Alaska eddies and associated anomalies. Deep-Sea Research I 54:487–509.

Lander, M. E., D. S. Johnson, J. T. Sterling, T. S. Gelatt, and B. S. Fadely. 2011*a*. Diving behaviors and movements of juvenile Steller sea lions (*Eumetopias jubatus*) captured in the central Aleutian Islands, April 2005. NOAA Technical Memorandum, NMFS–AFSC–218. National Marine Fisheries Service, Alaska Fisheries Science Center, Seattle, Washington, USA.

Lander, M. E., T. Lindstrom, M. Rutishausser, A. Franzheim, and M. Holland. 2015. Development and field testing a satellite-linked fluorometer for marine vertebrates. Animal Biotelemetry 3:40.

Lander, M. E., M. G. Logsdon, T. R. Loughlin, and G. R. VanBlaricom. 2011*b*. Spatial patterns and scaling behaviors of Steller sea lion (*Eumetopias jubatus*) distributions and their environment. Journal of Theoretical Biology 274:754–783.

Lander, M. E., T. R. Loughlin, M. G. Logsdon, G. R. VanBlaricom, and B. S. Fadely. 2010. Foraging effort of juvenile Steller sea lions (*Eumetopias jubatus*) with respect to heterogeneity of sea surface temperature. Endangered Species Research 10:145–158.

Lander, M. E., T. R. Loughlin, M. G. Logsdon, G. R. VanBlaricom, B. S. Fadely, and L. W. Fritz. 2009. Regional differences in the spatial and temporal heterogeneity of oceanographic habitat used by Steller sea lions. Ecological Applications 19:1645–1659.

Lauth, R. L., J. Guthridge, D. Nichol, S. W. McEntire, and N. Hillgruber. 2007*a*. Timing and duration of mating and brooding periods of Atka mackerel (*Pleurogrammus monopterygius*) in the North Pacific Ocean. Fishery Bulletin 105:560–570.

Lauth, R. L., S. W. McEntire, and H. H. Zenger Jr. 2007*b*. Geographic distribution, depth range, and description of Atka mackerel *Pleurogrammus monopterygius* nesting habitat in Alaska. Alaska Fishery Research Bulletin 12:165–186.

Laver, P. N., and M. J. Kelly. 2008. A critical review of home range studies. Journal of Wildlife Management 72:290–298.

Lea, M. A., D. Johnson, S. Melin, R. Ream, and T. Gelatt. 2010. Diving ontogeny and lunar responses in a highly migratory mammal, the northern fur seal (*Callorhinus ursinus)*. Marine Ecology Progress Series 419:233–247.

Loughlin, T. R. 1997. Using the phylogeographic method to identify Steller sea lion stocks. Pages 159–171 *in* A. E. Dizon, S. J. Chivers, and W. F. Perrin, editors. Molecular genetics of marine mammals. Special Publication Number 3. Allen Press, Inc., Lawrence, Kansas, USA.

Loughlin, T. R., A. S. Perlov, J. D. Baker, S. A. Blokhin, and A. G. Makhnyr. 1998. Diving behavior of adult female Steller sea lions in the Kuril Islands, Russia. Biosphere Conservation 1:21–31.

Loughlin, T. R., A. S. Perlov, and V. A. Vladimirov. 1992. Range-wide survey and estimation of total number of Steller sea lions in 1989. Marine Mammal Science 8:220–239.

Loughlin, T. R., and T. Spraker. 1989. Use of Telazol® to immobilize female northern sea lions (*Eumetopias jubatus*) in Alaska. Journal of Wildlife Diseases 25:353–358.

Loughlin, T. R., J. T. Sterling, R. Merrick, J. L. Sease, and A. E. York. 2003. Diving behavior of immature Steller sea lions (*Eumetopias jubatus*). Fishery Bulletin 101:566–582.

Loughlin, T. R., and A. E. York. 2000. An accounting of the sources of Steller sea lion, *Eumetopias jubatus*, mortality. Marine Fisheries Review 62:40–45.

Lowe, S. A., D. M. Van Doornik, and G. A. Winans. 1998. Geographic variation in genetic and growth patterns of Atka mackerel, *Pleurogrammus monopterygius* (Hexagrammidae), in the Aleutian archipelago. Fishery Bulletin 96:502–515.

Maniscalco, J. M., A. M. Springer, and P. Parker. 2010. High natality rates of endangered Steller sea lions in Kenai Fjords, Alaska and perceptions of population status in the Gulf of Alaska. PLOS ONE 10: e0140982.

Maslowski, W., J. C. Kinney, S. R. Okkonen, R. Osinski, A. F. Roberts, and W. J. Williams. 2014. The large scale ocean circulation and physical processes controlling Pacific-Arctic interactions. Pages 101–132 *in* J. M. Grebmeier and W. Maslowski, editors. The Pacific Arctic region: ecosystem status and trends in a rapidly changing environment. Springer, Dordrecht, The Netherlands.

Mayor, S. J., D. C. Schneider, J. A. Schaefer, and S. P. Mahoney. 2009. Habitat selection at multiple scales. Ecoscience 16:238–247.

McDermott, S. F., V. Haist, and K. M. Rand. 2016. Evaluating the efficacy of trawl exclusion zones by estimating local Atka mackerel abundance and movement patterns in the central and eastern Aleutian Islands. Marine and Coastal Fisheries 8:334–349.

McDermott, S. F., and S. A. Lowe. 1997. The reproductive cycle of Atka mackerel (*Pleurogrammus monopterygius*) in Alaska waters. Fishery Bulletin 95:231–333.

McDermott, S. F., K. Rand, M. Levine, J. A. Ianelli, E. A. Logerwell, and T. L. Loomis. 2014. Small-scale Atka mackerel population abundance and movement in the western Aleutian Islands, an area of continuing Steller sea lion decline. North Pacific Research Board project 1007 Final Report. https://workspace.aoos.org/published/file/ce

567153-9752-417f-8ffc-3ae5c5b559fe/1007%20Final%20report_1Oct14.pdf

McGarigal, K., H. Y. Wan, K. A. Zeller, B. C. Timm, and S. A. Cushman. 2016. Multi-scale habitat selection modeling: a review and outlook. Landscape Ecology 31:1161–1175.

McHuron, E. A., P. W. Robinson, S. E. Simmons, C. E. Kuhn, M. Fowler, and D. P. Costa. 2016. Foraging strategies of a generalist marine predator inhabiting a dynamic environment. Oecologia 182:995–1005.

McPherson, S., D. Bernard, J. H. Clark, K. Pahlke, E. Jones, J. Der Hovanisian, J. Weller, and R. Ericksen. 2004. Chinook salmon: status and escapement goals for stocks in Southeast Alaska. Pages 1–84 *in* H. J. Geiger and S. McPherson, editors. Stock status and escapement goals for salmon stocks in Southeast Alaska. Special Publication No. 04–02. Alaska Department of Fish and Game, Divisions of Sport Fish and Commercial Fisheries, Anchorage, Alaska, USA.

Mecklenburg, C. W., T. A. Mecklenburg, and L. K. Thorsteinson. 2002. Fishes of Alaska. American Fisheries Society, Bethesda, Maryland, USA.

Melin, S. R., M. Haulena, W. Van Bonn, M. J. Tennis, R. F. Brown, and J. D. Harris. 2013. Reversible immobilization of free-ranging adult male California sea lions (*Zalophus californianus*). Marine Mammal Science 29:E529–E536.

Merrick, R. L. 1995. The relationship of the foraging ecology of Steller sea lions (*Eumetopias jubatus*) to their population decline in Alaska. Dissertation. University of Washington, Seattle, Washington, USA.

Merrick, R. L., and T. R. Loughlin. 1997. Foraging behavior of adult female and young-of-the-year Steller sea lions in Alaskan waters. Canadian Journal of Zoology 75:776–786.

Merrick, R. L., T. R. Loughlin, G. A. Antonelis, and R. Hill. 1994. Use of satellite-linked telemetry to study Steller sea lion and northern fur seal foraging. Polar Research 13:105–114.

Merrick, R. L., T. R. Loughlin, and D. G. Calkins. 1987. Decline in abundance of the northern sea lion, *Eumetopias jubatus*, in Alaska, 1956–86. Fishery Bulletin 85:351–365.

Miller, A. J., et al. 2005. Interdecadal changes in mesoscale eddy variance in the Gulf of Alaska circulation: possible implications for the Steller sea lion decline. Atmosphere-Ocean 43:231–240.

Miyashita, K., K. Tetsumura, S. Honda, T. Oshima, R. Kawabe, and K. Sasaki. 2004. Diel changes in vertical distribution patterns of zooplankton and walleye pollock (*Theragra chalcogramma*) off the Pacific coast of eastern Hokkaido, Japan, estimated by the volume backscattering strength (Sv) method. Fisheries Oceanography 13:99–110.

Myers, K. W., N. V. Klovach, O. F. Gritsenko, S. Urawa, and T. C. Royer. 2007. Stock-specific distributions of Asian and North American salmon in the open ocean, interannual changes, and oceanographic conditions. North Pacific Anadromous Fish Commission Bulletin 4:159–177.

Neidetcher, S. K., T. P. Hurst, L. Ciannelli, and E. A. Logerwell. 2014. Spawning phenology and geography of Aleutian Islands and eastern Bering Sea Pacific cod (*Gadus macrocephalus*). Deep Sea Research Part II 109:204–214.

Neilson, J., and R. I. Perry. 1990. Diel vertical migration of fishes: an obligate or facultative process. Advances in Marine Biology 26:115–168.

Nichol, D. G., T. Honkalehto, and G. G. Thompson. 2007. Proximity of Pacific cod to the sea floor: using archival tags to estimate fish availability to research bottom trawls. Fisheries Research 86:129–135.

Nichol, D. G., S. Kotwicki, and M. Zimmermann. 2013. Diel vertical migration of adult Pacific cod *Gadus macrocephalus* in Alaska. Journal of Fish Biology 83:170–189.

Nichol, D. G., and D. A. Somerton. 2002. Diurnal vertical migration of the Atka mackerel *Pleurogrammus monopterygius* as shown by archival tags. Marine Ecology Progress Series 239:193–207.

NMFS [National Marine Fisheries Service]. 2001. Steller sea lion protection measures: final supplemental environmental impact statement (2). NOAA/NMFS, Juneau, Alaska, USA.

NMFS [National Marine Fisheries Service]. 2008. Recovery plan for the Steller sea lion: eastern and western distinct population segments (*Eumetopias jubatus*). Revision. NOAA/NMFS, Silver Spring, Maryland, USA. https://repository.library.noaa.gov/view/noaa/15974

NMFS [National Marine Fisheries Service]. 2014. Endangered Species Act Section 7 Biological Opinion: authorization of the Alaska groundfish fisheries under the proposed revised Steller sea lion protection measures. NOAA/NMFS, Juneau, Alaska, USA. https://repository.library.noaa.gov/view/noaa/17196

Nordstrom, C. A., B. C. Battaile, C. Cotte′, and A. W. Trites. 2013. Foraging habitats of lactating northern fur seals are structured by thermocline depths and submesoscale fronts in the eastern Bering Sea. Deep Sea Research Part II 88–89:78–96.

NRC [National Research Council]. 2003. Decline of the Steller sea lion in Alaskan waters: untangling food webs and fishing nets. The National Academies Press, Washington, D.C., USA.

Ogura, M., and Y. Ishida. 1992. Swimming behavior of coho salmon, *Oncorhynchus kisutch*, in the open sea as determined by ultrasonic telemetry. Canadian Journal of Fisheries and Aquatic Sciences 49:453–457.

Okkonen, S. R. 1996. The influence of an Alaskan Stream eddy on flow through Amchitka Pass. Journal of Geophysical Research 101:8839–8852.

Okkonen, S. R., G. A. Jacobs, E. J. Metzger, H. E. Hurlburt, and J. F. Shriver. 2001. Mesoscale variability in the boundary currents of the Alaska Gyre. Continental Shelf Research 21:1219–1236.

Okubo, A. 1970. Horizontal dispersion of floatable particles in the vicinity of velocity singularity such as convergences. Deep Sea Research and Oceanographic Abstracts 17:445–454.

Orians, G. H., and N. E. Pearson. 1979. On the theory of central place foraging. Pages 155–157 *in* D. J. Horn, G. R. Stairs, and R. D. Mitchell, editors. Analysis of ecological systems. Ohio State University Press, Columbus, Ohio, USA.

Orlov, A. M. 2003. Impact of eddies on spatial distributions of groundfishes along waters off the northern Kuril Islands, and southeastern Kamchatka (north Pacific Ocean). Indian Journal of Marine Sciences 32:95–113.

Orlov, A. M., and A. M. Tokranov. 2008. Specific features of distribution, some features of biology, and the dynamics of catches of smooth lumpsucker *Aptocyclus ventricosus* (Cyclopteridae) in waters of the Pacific Ocean off the Kuril Islands and Kamchatka. Journal of Ichthyology 48:86–101.

Paluszkiewicz, T., and H. J. Niebauer. 1984. Satellite observations of circulation in the eastern Bering Sea. Journal of Geophysical Research 89:3663–3678.

Pascual, M. A., and M. D. Adkison. 1994. The decline of the Steller sea lion in the Northeast Pacific: Demography, harvest or environment? Ecological Applications 4:393–403.

Pelland, N. A., J. T. Sterling, M. Lea, N. A. Bond, R. Ream, C. M. Lee, and C. C. Eriksen. 2014. Fortuitous encounters between seagliders and adult female northern fur seals (*Callorhinus ursinus*) off the Washington (USA) coast: upper ocean variability and links to top predator behavior. PLOS ONE 9:e101268.

Pitcher, K. W., D. G. Calkins, and G. W. Pendleton. 1998. Reproductive performance of female Steller sea lions: An energetics-based reproductive strategy? Canadian Journal of Zoology 76:2075–2083.

R Development Core Team. 2016. R: a language and environment for statistical computing. R Foundation for Statistical Computing, Vienna, Austria.

Rand, K. M., and S. A. Lowe. 2011. Defining essential fish habitat for Atka mackerel with respect to feeding within and adjacent to Aleutian Islands trawl exclusion zones. Marine and Coastal Fisheries 3:21–31.

Rand, K. M., P. Munro, S. K. Neidetcher, and D. G. Nichol. 2014. Observations of seasonal movement from a single tag release group of Pacific cod in the eastern Bering Sea. Marine and Coastal Fisheries 6:287–296.

Raum-Suryan, K. L., M. J. Rehberg, G. W. Pendleton, K. W. Pitcher, and T. S. Gelatt. 2004. Development of dispersal, movement patterns, and haul-out use by pup and juvenile Steller sea lions (*Eumetopias jubatus*) in Alaska. Marine Mammal Science 20:823–850.

Ream, R. R., J. T. Sterling, and T. R. Loughlin. 2005. Oceanographic features related to northern fur seal migratory movements. Deep-Sea Research Part II 52:823–843.

Rehberg, M. J., R. D. Andrews, U. G. Swain, and D. G. Calkins. 2009. Foraging behavior of adult female Steller sea lions during the breeding season in Southeast Alaska. Marine Mammal Science 25:588–604.

Reuter, R., and T. Tenbrink. 2008. Assessment of sculpin stocks in the eastern Bering Sea and Aleutian Islands. Pages 1409–1448 *in* Stock assessment and fishery evaluation report of the groundfish resources of the Bering Sea and Aleutian Islands region. North Pacific Fishery Management Council, Anchorage, Alaska, USA. https://www.afsc.noaa.gov/refm/docs/2008/BSAIsculpin.pdf

Rooper, C., and J. L. Boldt. 2005. Distribution of juvenile Pacific ocean perch (*Sebastes alutus*) in the Aleutian Islands in relation to benthic habitat. Alaska Fisheries Research Bulletin 11:102–112.

Rooper, C., and M. Zimmermann. 2007. A bottom-up methodology for integrating underwater video and acoustic mapping for seafloor classification. Continental Shelf Research 27:947–957.

Rosen, D. A. S. 2009. Steller sea lions *Eumetopias jubatus* and nutritional stress: evidence from captive studies. Mammal Review 39:284–306.

Samuel, M. D., D. J. Pierce, and E. O. Garton. 1985. Identifying areas of concentrated use within the home range. Journal of Animal Ecology 54:711–719.

Scherer, R. D., A. C. Doll, L. D. Rea, A. M. Christ, C. A. Stricker, B. Witteveen, T. C. Kline, C. M. Kurle, and M. B. Wunder. 2015. Stable isotope values in pup vibrissae reveal geographic variation in diets of gestating Steller sea lions *Eumetopias jubatus*. Marine Ecology Progress Series 527:261–274.

Sigler, M. F., and D. J. Csepp. 2007. Seasonal abundance of two important forage species in the North Pacific Ocean, Pacific herring and walleye pollock. Fisheries Research 83:319–331.

Sigler, M. F., D. J. Tollit, J. J. Vollenweider, J. F. Thedinga, D. J. Csepp, J. N. Womble, M. A. Wong, M. J. Rehberg, and A. W. Trites. 2009. Steller sea lion foraging response to seasonal changes in prey availability. Marine Ecology Progress Series 388:243–261.

Sigler, M. F., J. N. Womble, and J. J. Vollenweider. 2004. Availability to Steller sea lions (*Eumetopias jubatus*) of a seasonal prey resource: a prespawning aggregation of eulachon (*Thaleichthys pacificus*). Canadian Journal of Fisheries and Aquatic Sciences 61:1475–1484.

Silber, G. K., et al. 2017. Projecting marine mammal distribution in a changing climate. Frontiers in Marine Science 4:413.

Simmons, S. E., D. E. Crocker, R. M. Kudela, and D. P. Costa. 2007. Linking foraging behavior of the northern elephant seal with oceanography and bathymetry at mesoscales. Marine Ecology Progress Series 346:265–275.

Sinclair, E. H., D. S. Johnson, T. K. Zeppelin, and T. S. Gelatt. 2013. Decadal variation in the diet of western stock Steller sea lions (*Eumetopias jubatus*). NOAA Technical Memorandum, NMFS–AFSC–248. National Marine Fisheries Service, Alaska Fisheries Science Center, Seattle, Washington, USA.

Sinclair, E. H., and T. K. Zeppelin. 2002. Seasonal and spatial differences in diet in the western stock of Steller sea lions. Journal of Mammalogy 83:973–990.

Spelman, L. H. 2004. Reversible anesthesia of captive California sea lions (*Zalophus californianus*) with Medetomidine, Midazolam, Butorphanol, and isoflurane. Journal of Zoo and Wildlife Medicine 35:65–69.

Stabeno, P. J., J. D. Schumacher, and K. Ohtani. 1999. The physical oceanography of the Bering Sea. Pages 1–28 *in* T. R. Loughlin and K. Ohtani, editors. Dynamics of the Bering Sea. AK–SG–99–03. University of Alaska Sea Grant, Fairbanks, Alaska, USA.

Sterling, J. T., A. M. Springer, S. J. Iverson, S. P. Johnson, N. A. Pelland, D. S. Johnson, M. Lea, and N. A. Bond. 2014. The sun, moon, wind, and biological imperative-shaping contrasting wintertime migration and foraging strategies of adult male and female northern fur seals (*Callorhinus ursinus*). PLOS ONE 9:e93068.

Tenbrink, T. T., and T. W. Buckley. 2013. Life-history aspects of the Yellow Irish Lord (*Hemilepidotus jordani*) in the eastern Bering Sea and Aleutian Islands. Northwestern Naturalist 94:126–136.

Thompson, D., C. D. Duck, B. J. McConnell, and J. Garrett. 1998. Foraging behavior and diet of lactating female southern sea lions (*Otaria flavescens*) in the Falkland Islands. Journal of Zoology London 246:135–146.

Tollit, D., L. Fritz, R. Joy, K. Miller, A. Schulze, J. Thomason, W. Walker, T. Zeppelin, and T. Gelatt. 2017. Diet of endangered Steller sea lions in the Aleutian Islands: new insights from DNA detections and bio-energetic reconstructions. Canadian Journal of Zoology 95:853–868.

Trites, A. W., and C. P. Donnelly. 2003. The decline of Steller sea lions *Eumetopias jubatus* in Alaska: a review of the nutritional stress hypothesis. Mammal Review 33:3–28.

Trites, A. W., B. P. Porter, V. B. Deecke, A. P. Coombs, M. L. Marcotte, and D. A. S. Rosen. 2006. Insights into the timing of weaning and the attendance patterns of lactating Steller sea lions (*Eumetopias jubatus*) in Alaska during winter, spring, and summer. Aquatic Mammals 32:85–97.

Trites, A. W., et al. 2007. Bottom-up forcing and the decline of Steller sea lions (*Eumetopias jubatus*) in Alaska: assessing the ocean climate hypothesis. Fisheries Oceanography 16:46–67.

Turner, M. G. 2005. Landscape ecology: What is the state of science? Annual Review of Ecology, Evolution, and Systematics 36:319–344.

Turner, K., C. N. Rooper, E. Laman, S. Rooney, D. Cooper, and M. Zimmerman. 2017. Model-based essential fish habitat definitions for Aleutian Island groundfish species. NOAA Technical Memorandum, NMFS–AFSC–360. National Marine Fisheries Service, Alaska Fisheries Science Center, Seattle, Washington, USA.

Ueno, H., H. J. Freeland, W. R. Crawford, H. Onishi, E. Oka, K. Sato, and T. Suga. 2008. Anticyclonic eddies in the Alaskan Stream. Journal of Physical Oceanography 39:934–951.

Van Winkle, W. 1975. Comparison of several probabilistic home-range models. Journal of Wildlife Management 39:118–123.

Ver Hoef, J. M., and P. L. Boveng. 2015. Iterating on a single model is a viable alternative to multimodel inference. Journal of Wildlife Management 79:719–729.

Vollenweider, J. J., R. A. Heintz, L. Schaufler, and R. Bradshaw. 2011. Seasonal cycles in whole-body proximate composition and energy content of forage fish vary with water depth. Marine Biology 158:413–427.

Waite, J. N., S. J. Trumble, V. N. Burkanov, and R. D. Andrews. 2012. Resource partitioning by sympatric Steller sea lions and northern fur seals as revealed by biochemical dietary analyses and satellite telemetry. Journal of Experimental Marine Biology and Ecology 416–417:41–54.

Walker, R. V., V. V. Sviridov, S. Urawa, and T. Azumaya. 2007. Spatio-temporal variation in vertical distributions of Pacific salmon in the ocean. North

Pacific Anadromous Fish Commission Bulletin 4:193–201.

Watanabe, H., T. Kubodera, M. Moku, and K. Kawaguchi. 2006. Diel vertical migration of squid in the warm core ring and cold water masses in the transition region of the western North Pacific. Marine Ecology Progress Series 315:187–197.

Watanabe, H., M. Moku, K. Kawaguchi, K. Ishimaru, and A. Ohno. 1999. Diel vertical migration of myctophid fishes (Family Myctophidae) in the transitional waters of the western North Pacific. Fisheries Oceanography 8:115–127.

Weiss, J. 1991. The dynamics of enstrophy transfer in two dimensional hydrodynamics. Physica D: Nonlinear Phenomena 48:273–294.

Wiens, J. A. 1989. Spatial scaling in ecology. Functional Ecology 3:385–397.

Willson, M. F., R. H. Armstrong, M. C. Hermans, and K. Koski. 2006. Eulachon: a review of biology and an annotated bibliography. AFSC Processed Report 2006–12. National Marine Fisheries Service, Alaska Fisheries Science Center, Juneau, Alaska, USA.

Wilson, K., E. Hanks, and D. Johnson. 2018. Estimating animal utilization densities using continuous-time Markov chain models. Methods in Ecology and Evolution 9:1232–1240.

Winship, A. J., and A. W. Trites. 2006. Risk of extirpation of Steller sea lions in the Gulf of Alaska and Aleutian Islands: a population viability analysis based on alternative hypotheses for why sea lions declined in western Alaska. Marine Mammal Science 22:124–155.

Womble, J. N. 2003. Seasonal distribution of Steller sea lions (*Eumetopias jubatus*) in relation to high-quality ephemeral prey species in southeastern Alaska. Thesis. University of Alaska Fairbanks, Fairbanks, Alaska, USA.

Womble, J. N., and M. F. Sigler. 2006. Seasonal availability of abundant, energy-rich prey influences the abundance and diet of a marine predator, the Steller sea lion *Eumetopias jubatus*. Marine Ecology Progress Series 325:281–293.

Womble, J. N., M. F. Sigler, and M. F. Willson. 2009. Linking seasonal distribution patterns with prey availability in a central-place forager, the Steller sea lion. Journal of Biogeography 36:439–451.

Womble, J. N., M. F. Willson, M. F. Sigler, B. P. Kelly, and G. R. VanBlaricom. 2005. Distribution of Steller sea lions *Eumetopias jubatus* in relation to spring-spawning fish in SE Alaska. Marine Ecology Progress Series 294:271–282.

Wood, S. N. 2006. Generalized additive models: an introduction with R. Chapman and Hall-CRC, Boca Raton, Florida, USA.

Wood, S. N. 2009. Mgcv. R package version 1.6-0. http://CRAN.R-project.org/package=mgcv

Wood, S. N. 2017. Generalized additive models: an introduction with R. Second edition. Chapman and Hall-CRC, Boca Raton, Florida, USA.

Wood, S. N., Y. Goude, and S. Shaw. 2015. Generalized additive models for large data sets. Applied Statistics C 64:139–155.

Worton, B. J. 1989. Kernel methods for estimating the utilization distribution in home-range studies. Ecology 70:164–168.

York, A. 1994. The population decline of northern sea lions, 1975–1985. Marine Mammal Science 10:38–51.

York, A. E., R. L. Merrick, and T. R. Loughlin. 1996. An analysis of the Steller sea lion Metapopulation in Alaska. Pages 259–292 *in* D. R. Cullough, editor. Metapopulations and wildlife conservation. Island Press, Washington, D.C., USA.

Zhukova, K., O. A. Maznikova, and A. M. Orlov. 2018. Gonadal maturation of the female lumpsucker (*Aptocyclus ventricosus*). Fishery Bulletin 116:153–160.

Zimmermann, M., and J. Benson. 2013. Smooth sheets: how to work with them in a GIS to derive bathymetry, features and substrates. NOAA Technical Memorandum, NMFS–AFSC–249. National Marine Fisheries Service, Alaska Fisheries Science Center, Seattle, Washington, USA.

Zimmermann, M., M. M. Prescott, and C. N. Rooper. 2013. Smooth sheet bathymetry of the Aleutian Islands. NOAA Technical Memorandum, NMFS–AFSC–250. National Marine Fisheries Service, Alaska Fisheries Science Center, Seattle, Washington, USA.

SUPPORTING INFORMATION

Additional Supporting Information may be found online at: http://onlinelibrary.wiley.com/doi/10.1002/ecs2.3021/full